Lehrstuhl für Regelungstechnik
Technical Reports on Automatic Control
Vol. TRAC-7, June 6, 2013
Available online at: www.rt.mw.tum.de
Technische Universität München

Energy Based Attitude Tracking Control for a Quadrotor Helicopter Prioritizing the Thrust Direction

Oliver Fritsch *
Lehrstuhl für Regelungstechnik, Technische Universität München
Boltzmannstr. 15, D-85748 Garching, Germany

Abstract

In this paper an energy based attitude tracking control for a quadrotor helicopter is presented. The controller can be considered as an extension of both the setpoint attitude control presented in [8] and the reduced attitude tracking controller from [7]. The controller prioritizes the alignment of the quadrotor's thrust axis due to its critical role for the translational dynamics. In contrast to [8], the whole control problem is reformulated using the rotation matrix to represent the attitude instead of quaternions. This way the ambiguity inherent to the quaternion representation is omitted. Global and local analysis of all equilibrium points of the tracking error dynamics is provided and shows that tracking of the desired attitude is achieved for almost all initial conditions. In detail, almost global asymptotic stability and local exponential stability is established for the equilibrium corresponding to a zero tracking error.

Keywords: Quadrotor attitude tracking; Energy shaping; Almost global asymptotic stability

1 Introduction

A quadrotor helicopter is a highly maneuverable vertical take-off and landing aircraft, which offers the ability of hovering. As shown in Fig. 1, it is basically a rigid body with four rotors arranged in a common plane which generate thrust forces and drag moments. The effects of the four single rotors can be summarized in the center of gravity as a total thrust F perpendicular to the plane and a torque vector $\boldsymbol{\tau} = \begin{bmatrix} \tau_x & \tau_y & \tau_z \end{bmatrix}^T$. Since the direction of the thrust is body-fixed, the execution of almost all translational motions requires tilting the whole quadrotor helicopter systematically. Consequently, a desired thrust direction is usually the output of a higher level position controller or the remote control command of a human operator. Additionally, a desired orientation of the quadrotor around its desired thrust axis can be specified. This can be done for example by defining a desired heading for one of the quadrotors arms in the horizontal plane. The resulting desired attitude has to be tracked by an appropriate attitude controller. Due to the significance of the thrust direction for the translational dynamics it plays a critical role in the attitude control task of a quadrotor and its alignment should be prioritized compared to the heading.

The control task belongs to the broad field of rigid body attitude control, which has been extensively studied for decades, especially in the context of spacecraft applications. A survey on the

*Corresponding author: Tel: +49 89 289 15670, Fax: +49 89 25915653, email: oliver.fritsch@tum.de

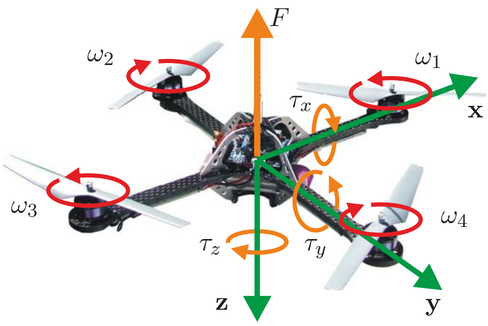

Figure 1: Quadrotor with body-fixed frame $B = \{\mathbf{x}, \mathbf{y}, \mathbf{z}\}$ and control inputs $F, \tau_x, \tau_y, \tau_z$.

topic was recently published in [5]. Also in the field of unmanned aerial vehicles like quadrotor helicopters the attitude control task has been intensively addressed, see e.g. [3, 6, 13, 16]. Significantly fewer works are concerned with reduced attitude control, which deals with the alignment of only one body axis. Some examples are [2, 4, 5, 10, 17]. The controller presented here, combines both control problems in the way that the alignment of one body axis is considerably prioritized. Although for quadrotor applications the significance of the thrust axis is obvious, to the best knowledge of the author, no attitude tracking control for a quadrotor helicopter prioritizing the thrust axis has been published so far. A saturating attitude setpoint control with these features was introduced by the author and others in [8].

The controller presented in this paper is based on an energy shaping approach (see e.g. [14]). It can be roughly assigned to the very general concept published in [4] but focuses on indicating explicit energy and damping functions. A suitable shaping of the closed loop energy and a sophisticated damping strategy lead to a fast transient behavior prioritizing the alignment of the thrust direction. The energy based controller design gives rise to a continuous state feedback law, which renders the equilibrium corresponding to a zero tracking error almost asymptotically and locally exponentially stable. The presented controller extends the attitude setpoint control proposed in [8] to an attitude tracking control by adding suitable feedforward terms to the control law. In addition, the potential energy functions proposed in [8] are slightly modified to facilitate the local analysis of the closed loop equilibrium points. At the same time, the influence of the modifications on the controller perfomance is negligible. Moreover, the control problem is restated using the rotation matrix for the attitude parametrization instead of quaternions. The ambiguity inherent to the quaternion representation can thus be omitted. Finally, the new attitude representation contributes to reveal that this paper can also be considered as a straight forward extension of the reduced attitude tracking controller presented in [7].

In Section 2 we briefly introduce the notation and the definitions used in the following. A detailed problem statement is given in Section 3. Some considerations concerning the computation of the heading command are discussed in Section 4 and in Section 5 the attitude tracking dynamics are derived. Based on an energy shaping approach, the control law is developed in Section 6, before the stability properties of the closed loop equilibrium points are thoroughly analyzed in Section 7. Finally, conclusions are drawn in Section 8.

2 Nomenclature and Definitions

Scalars are indicated as italic letters, whereas vectors, matrices and composite quantities are indicated by upright bold letters. Any physical vector $\mathbf{a} \in \mathbb{R}^3$ has meaning even without concrete numerical values and is thus referred to as an abstract vector. To assign numerical values to an abstract vector a suitable coordinate frame has to be chosen. All coordinate frames used are right-handed Cartesian coordinate systems and identified by uppercase italic letters. The representation of an abstract vector $\mathbf{a} \in \mathbb{R}^3$ with respect to a certain frame $E = \{\mathbf{e}_1, \mathbf{e}_2, \mathbf{e}_3\}$ with orthonormal basis vectors $\mathbf{e}_1, \mathbf{e}_2, \mathbf{e}_3$ is denoted by $\mathbf{a}_E$. The elements of a vector $\mathbf{a}_E$ are identified by $\mathbf{a}_E = \begin{bmatrix} a_{Ex} & a_{Ey} & a_{Ez} \end{bmatrix}^T$ and by $\mathbf{a}_{Exy}$ we mean $\mathbf{a}_{Exy} = \begin{bmatrix} a_{Ex} & a_{Ey} \end{bmatrix}^T$. For some vectors, which are exclusively represented in one coordinate frame, the basis designation will be dropped. Additionally, we define the basis independent unit vectors $\mathbf{e}_x = \begin{bmatrix} 1 & 0 & 0 \end{bmatrix}^T$, $\mathbf{e}_y = \begin{bmatrix} 0 & 1 & 0 \end{bmatrix}^T$ and $\mathbf{e}_z = \begin{bmatrix} 0 & 0 & 1 \end{bmatrix}^T$. The transformation from a frame E to another frame E' is given by a rotation matrix $\mathbf{R}_{E'E} \in SO(3)$, where $SO(3) = \{\mathbf{R} \in \mathbb{R}^{3\times 3} : \mathbf{R}^T\mathbf{R} = \mathbf{I}_3, \det(\mathbf{R}) = 1\}$ is the special orthogonal group and $\mathbf{I}_i$, $i \in \mathbb{N}$ denotes the $i \times i$ identity matrix. The angular velocity of a frame E' with respect to a frame E given in a frame E'' is denoted by $\boldsymbol{\omega}_{E''}^{EE'} \in \mathbb{R}^3$. The skew symmetric operator $\langle\!\langle \cdot \rangle\!\rangle : \mathbb{R}^3 \to \mathfrak{so}(3)$, where $\mathfrak{so}(3) = \{\mathbf{K} \in \mathbb{R}^{3\times 3} : \mathbf{K}^T = -\mathbf{K}\}$ is defined such that $\langle\!\langle \mathbf{a} \rangle\!\rangle \mathbf{b} = \mathbf{a} \times \mathbf{b}$ reflects the cross product for $\mathbf{a}, \mathbf{b} \in \mathbb{R}^3$. The inverse operator is $\rangle\!\rangle \cdot \langle\!\langle : \mathfrak{so}(3) \to \mathbb{R}^3$. The unit sphere of dimension $i \in \mathbb{N}$ is denoted by $\mathcal{S}^i = \{\mathbf{a} \in \mathbb{R}^{i+1} : \mathbf{a}^T\mathbf{a} = 1\}$. We will also make use of the following functions: By $\Lambda_{\zeta_l}^{\zeta_u} : [0, \pi] \to [0, \sin(\zeta_l)]$ we denote the function

$$\Lambda_{\zeta_l}^{\zeta_u}(\zeta) = \begin{cases} \sin(\zeta) & \text{if} \quad 0 \le \zeta \le \zeta_l \,, \\ \sin(\zeta_l) & \text{if} \quad \zeta_l < \zeta \le \zeta_u \,, \\ \frac{\sin(\zeta_l)}{\sin(\zeta_u)} \sin(\zeta) & \text{if} \quad \zeta_u < \zeta \le \pi \,, \end{cases} \tag{1}$$

where $\zeta_l, \zeta_u \in \mathbb{R}_+$ are constants. Furthermore, we use the function $\chi_{\zeta_1}^{\zeta_2} : \mathbb{R} \times \mathbb{R} \times \mathbb{R} \to \mathbb{R}$,

$$\chi_{\zeta_1}^{\zeta_2}(\zeta, \psi_1(\zeta, \mathbf{a}), \psi_2(\zeta, \mathbf{a})) = \begin{cases} \psi_1(\zeta, \mathbf{a}) & \text{if } \zeta \le \zeta_1 \,, \\ \frac{(\zeta_2 - \zeta)\psi_1(\zeta_1, \mathbf{a}) + (\zeta - \zeta_1)\psi_2(\zeta_2, \mathbf{a})}{\zeta_2 - \zeta_1} & \text{if } \zeta_1 < \zeta \le \zeta_2 \,, \\ \psi_2(\zeta, \mathbf{a}) & \text{if } \zeta_2 < \zeta \,, \end{cases} \tag{2}$$

which provides a linear interpolation between the scalar functions $\psi_1(\zeta, \mathbf{a})$ and $\psi_2(\zeta, \mathbf{a})$ with respect to ζ in the interpolation region defined by ζ_1 and ζ_2. For some $\zeta_1 < \zeta_2 < \zeta_3 < \zeta_4$ we moreover define

$$\chi_{\zeta_1, \zeta_2}^{\zeta_3, \zeta_4}(\zeta, \psi_1(\zeta, \mathbf{a}), \psi_2(\zeta, \mathbf{a})) \coloneqq \chi_{\zeta_1}^{\zeta_2}\left(\zeta, \psi_1(\zeta, \mathbf{a}), \chi_{\zeta_3}^{\zeta_4}(\zeta, \psi_2(\zeta, \mathbf{a}), \psi_1(\zeta, \mathbf{a}))\right) , \tag{3}$$

which provides a linear interpolation from $\psi_1(\zeta, \mathbf{a})$ to $\psi_2(\zeta, \mathbf{a})$ and back to $\psi_1(\zeta, \mathbf{a})$.

We will frequently encounter the case that a (scalar, vector or matrix) quantity a can be given as a function $f(\cdot)$ of coordinates $\mathbf{b}$, i.e. $a = f(\mathbf{b})$, and also as a function $\tilde{f}(\cdot)$ of coordinates $\mathbf{c}$, i.e. $a = \tilde{f}(\mathbf{c})$. With a slight abuse of notation we will write $a(\mathbf{b})$ to refer to $f(\mathbf{b})$ and $a(\mathbf{c})$ to refer to $\tilde{f}(\mathbf{c})$. Sometimes, we will also drop the argument and in that case writing a may refer to $f(\mathbf{b})$ or $\tilde{f}(\mathbf{c})$ depending on the context.

Finally, some properties of the skew symmetric operator $\langle\!\langle \cdot \rangle\!\rangle$ that will be needed in the following are stated. They can be found for example in [15]. By the skew symmetry it holds that $\langle\!\langle \mathbf{a} \rangle\!\rangle = -\langle\!\langle \mathbf{a} \rangle\!\rangle^T$. Since $\langle\!\langle \mathbf{a} \rangle\!\rangle \mathbf{b}$ reflects the cross product $\mathbf{a} \times \mathbf{b}$ we also have that $\langle\!\langle \mathbf{a} \rangle\!\rangle \mathbf{b} = -\langle\!\langle \mathbf{b} \rangle\!\rangle \mathbf{a}$. Moreover, for any rotation matrix $\mathbf{R}_{E'E}$ and any vector $\mathbf{a} \in \mathbb{R}^3$ it holds that

$$\mathbf{R}_{E'E} \langle\!\langle \mathbf{a} \rangle\!\rangle \mathbf{R}_{E'E}^T = \langle\!\langle \mathbf{R}_{E'E} \mathbf{a} \rangle\!\rangle \,. \tag{4}$$

3 Problem Statement

Regarding the attitude, we model the quadrotor helicopter as a rigid body actuated in torque. This commonly used model exploits the generally accepted assumption that there exists a known one to one relation $\begin{bmatrix} F & \boldsymbol{\tau}^T \end{bmatrix}^T = \mathbf{f}(\omega_1^2, \omega_2^2, \omega_3^2, \omega_4^2)$ (see e.g. [16]) between the magnitude F of the thrust force, the torque vector $\boldsymbol{\tau}$ and the squares of the rotor angular rates ω_i, $i \in \{1, 2, 3, 4\}$, which are the real control variables. Furthermore, the model neglects some minor effects like the gyroscopic torques of the rotors or the flapping dynamics. We distinguish an inertial north east down coordinate frame $I = \{\mathbf{e}_{north}, \mathbf{e}_{east}, \mathbf{e}_{down}\}$ and a body-fixed frame $B = \{\mathbf{x}, \mathbf{y}, \mathbf{z}\}$ attached to the center of gravity of the quadrotor and oriented as shown in Fig. 1. Then, the rigid body attitude dynamics read

$$\dot{\mathbf{R}}_{BI} = -\langle\!\langle \boldsymbol{\omega}_B^{IB} \rangle\!\rangle \mathbf{R}_{BI} \,, \tag{5}$$

$$\mathbf{J}\dot{\boldsymbol{\omega}}_B^{IB} = -\langle\!\langle \boldsymbol{\omega}_B^{IB} \rangle\!\rangle \mathbf{J}\boldsymbol{\omega}_B^{IB} + \boldsymbol{\tau} \,, \tag{6}$$

where $\mathbf{J} = \mathbf{J}^T > \mathbf{0}$ is the moment of inertia matrix given in B and $\boldsymbol{\tau} = \boldsymbol{\tau}_B$ is the control torque. In the following we assume that the states $\mathbf{R}_{BI}$ and $\boldsymbol{\omega}_B^{IB}$ are accessible either by direct measurements or as the output of an appropriate data fusion.

The control objective is to make the body-fixed frame $B = \{\mathbf{x}, \mathbf{y}, \mathbf{z}\}$ track a desired time-varying frame $D = \{\mathbf{x}_d, \mathbf{y}_d, \mathbf{z}_d\}$, or in terms of rotation matrices $\mathbf{R}_{BI} \to \mathbf{R}_{DI}$ as $t \to \infty$. Regarding the error rotation matrix $\mathbf{R}_{BD} = \mathbf{R}_{BI}\mathbf{R}_{ID} = \mathbf{R}_{BI}\mathbf{R}_{DI}^T$ the objective reads $\mathbf{R}_{BD} \to \mathbf{I}_3$ as $t \to \infty$.

The translational dynamics of a quadrotor can be manipulated only along the body-fixed z-axis, since the thrust vector always points in the direction $-\mathbf{z}$. Hence, a higher level position controller usually provides the desired z-axis direction $\mathbf{z}_d$ in its inertial representation $\mathbf{z}_{dI}$ as well as its time derivatives $\dot{\mathbf{z}}_{dI}, \ddot{\mathbf{z}}_{dI}$. Additionally, $\mathbf{x}_{dI}, \dot{\mathbf{x}}_{dI}$ and $\ddot{\mathbf{x}}_{dI}$ can be computed from a known heading command as shown in Section 4. As $\mathbf{y}_{dI} = \langle\!\langle \mathbf{z}_{dI} \rangle\!\rangle \mathbf{x}_{dI}$ holds, the desired frame D and its evolution with respect to time is completely defined by the known command signals. Regarding the rotation matrix $\mathbf{R}_{ID}$ it holds that

$$\begin{aligned} \mathbf{R}_{ID} &= \begin{bmatrix} \mathbf{x}_{dI} & \langle\!\langle \mathbf{z}_{dI} \rangle\!\rangle \mathbf{x}_{dI} & \mathbf{z}_{dI} \end{bmatrix} , \quad \dot{\mathbf{R}}_{ID} = \begin{bmatrix} \dot{\mathbf{x}}_{dI} & \langle\!\langle \dot{\mathbf{z}}_{dI} \rangle\!\rangle \mathbf{x}_{dI} + \langle\!\langle \mathbf{z}_{dI} \rangle\!\rangle \dot{\mathbf{x}}_{dI} & \dot{\mathbf{z}}_{dI} \end{bmatrix} , \\ \ddot{\mathbf{R}}_{ID} &= \begin{bmatrix} \ddot{\mathbf{x}}_{dI} & \langle\!\langle \ddot{\mathbf{z}}_{dI} \rangle\!\rangle \mathbf{x}_{dI} + 2\langle\!\langle \dot{\mathbf{z}}_{dI} \rangle\!\rangle \dot{\mathbf{x}}_{dI} + \langle\!\langle \mathbf{z}_{dI} \rangle\!\rangle \ddot{\mathbf{x}}_{dI} & \ddot{\mathbf{z}}_{dI} \end{bmatrix} . \end{aligned} \tag{7}$$

It proves advantageous to decompose the transpose of the error rotation matrix $\mathbf{R}_{BD}^T = \mathbf{R}_{DB}$ into two particular rotations, $\mathbf{R}_{DB} = \mathbf{R}_{DA}\mathbf{R}_{AB}$. This is illustrated in Figure 2. The first rotation $\mathbf{R}_{AB}$ is about an axis $\mathbf{e}_\varphi$ in the body-fixed xy-plane through an angle φ and transforms into an auxiliary frame $A = \{\mathbf{x}_a, \mathbf{y}_a, \mathbf{z}_d\}$. The rotation is such that the z-axis of A coincides with the desired direction $\mathbf{z}_d$. It immediately follows that $\mathbf{e}_\varphi$ is defined by the normalized cross product of $\mathbf{z}$ and $\mathbf{z}_d$,

$$\mathbf{e}_{\varphi B} = \frac{1}{\|\langle\!\langle \mathbf{z}_B \rangle\!\rangle \mathbf{z}_{dB}\|} \langle\!\langle \mathbf{z}_B \rangle\!\rangle \mathbf{z}_{dB} = \frac{1}{\|\langle\!\langle \mathbf{e}_z \rangle\!\rangle \mathbf{z}_{dB}\|} \langle\!\langle \mathbf{e}_z \rangle\!\rangle \mathbf{z}_{dB} = \frac{1}{\sqrt{z_{dBx}^2 + z_{dBy}^2}} \begin{bmatrix} -z_{dBy} \\ z_{dBx} \\ 0 \end{bmatrix} . \tag{8}$$

The corresponding rotation angle is $\varphi = \arccos(\mathbf{e}_z^T \mathbf{z}_{dB}) = \arccos(z_{dBz}) \in [0, \pi]$. Since we will use $\mathbf{e}_\varphi$ only in the body-fixed representation, the index B will be dropped in the following such that $\mathbf{e}_\varphi = \mathbf{e}_{\varphi B}$ holds. Finally, the second matrix $\mathbf{R}_{DA}$ describes the remaining rotation from A to D about an axis parallel or antiparallel to their common z-axis $\mathbf{z}_d$. The rotation is through an angle ϑ and can obviously be computed by $\vartheta = \arccos(\mathbf{x}_{aA}^T \mathbf{x}_{dA}) = \arccos(\mathbf{e}_x^T \mathbf{x}_{dA}) = \arccos(x_{dAx}) \in [0, \pi]$. Since A and D have a common z-axis it moreover holds that $x_{dAz} \equiv 0$ and thus it suffices to consider the reduced vector $\mathbf{x}_{dAxy}$ to specify $\mathbf{x}_{dA}$. Apart from some exceptions discussed in Remark 1, $\mathbf{R}_{AB}$ and $\mathbf{R}_{DA}$ are completely defined by the vectors $\mathbf{z}_{dB}$ and $\mathbf{x}_{dAxy}$ and hence they represent an appropriate parametrization of the error rotation matrix $\mathbf{R}_{BD}$, which is the natural attitude error state. More technically speaking there exists a local (but

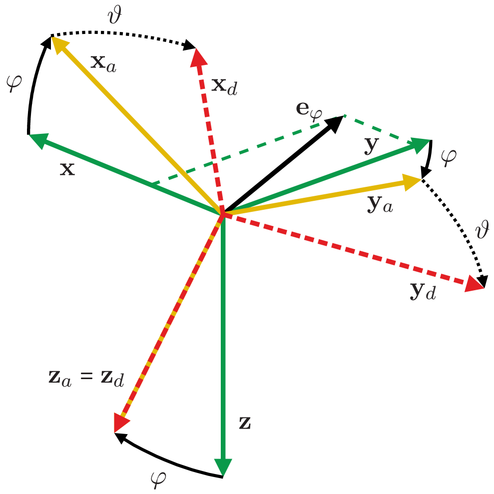

Figure 2: Decomposition of the attitude error into two successive rotations: First, from the body-fixed frame $B = \{\mathbf{x}, \mathbf{y}, \mathbf{z}\}$ to the auxiliary frame $A = \{\mathbf{x}_a, \mathbf{y}_a, \mathbf{z}_a\}$. Second, from A to the desired frame $D = \{\mathbf{x}_d, \mathbf{y}_d, \mathbf{z}_d\}$.

almost global) diffeomorphism between $\mathbf{z}_{dB}$, $\mathbf{x}_{dAxy}$ and $\mathbf{R}_{BD}$. Careful treatment of the fact that the diffeomorphism is only local enables us to largely use $\mathbf{z}_{dB} \in \mathcal{S}^2 = \{\mathbf{a} \in \mathbb{R}^3 : \mathbf{a}^T\mathbf{a} = 1\}$ as a representation of the thrust direction error and $\mathbf{x}_{dAxy} \in \mathcal{S} = \{\mathbf{a} \in \mathbb{R}^2 : \mathbf{a}^T\mathbf{a} = 1\}$ as a representation of the heading error anyway. In terms of $\mathbf{z}_{dB}$ and $\mathbf{x}_{dAxy}$ the control objective is $\mathbf{z}_{dB} \to \mathbf{e}_z$ and $\mathbf{x}_{dAxy} \to \begin{bmatrix}1 & 0\end{bmatrix}^T$ as $t \to \infty$. As the translational dynamics can be manipulated only in the thrust direction, the alignment of the thrust is of higher importance than the alignment of the remaining axes. We consider this in the design process by constructing a control law that focuses on $\mathbf{z}_{dB} \to \mathbf{e}_z$.

4 Computation Of the Heading Command

The desired heading is specified by a time-varying unit vector $\mathbf{h} \in \mathcal{S}^2$ lying in the horizontal plane spanned by $\mathbf{e}_{north}$ and $\mathbf{e}_{east}$. The time derivatives $\dot{\mathbf{h}}$ and $\ddot{\mathbf{h}}$ are assumed to be known and bounded. The desired x-axis direction $\mathbf{x}_d$ is now obtained by the normalized projection of $\mathbf{h}$ along $\mathbf{e}_{down}$ onto the plane perpendicular to $\mathbf{z}_d$. This projection always exists as long as $\mathbf{z}_d$ does not lie within the horizontal plane itself. Noting that $\mathbf{e}_{down\,I} = \mathbf{e}_z$, we obtain

$$\mathbf{x}_{dI} = \frac{1}{\|\langle\!\langle\langle\!\langle \mathbf{e}_z\rangle\!\rangle \mathbf{h}_I\rangle\!\rangle \mathbf{z}_{dI}\|}\langle\!\langle\langle\!\langle \mathbf{e}_z\rangle\!\rangle \mathbf{h}_I\rangle\!\rangle \mathbf{z}_{dI} = \frac{-1}{\sqrt{\mathbf{h}_I^T\langle\!\langle \mathbf{e}_z\rangle\!\rangle\langle\!\langle \mathbf{z}_{dI}\rangle\!\rangle^2\langle\!\langle \mathbf{e}_z\rangle\!\rangle \mathbf{h}_I}}\langle\!\langle \mathbf{z}_{dI}\rangle\!\rangle\langle\!\langle \mathbf{e}_z\rangle\!\rangle \mathbf{h}_I \tag{9}$$

and computation of the time derivatives yields

$$\begin{aligned}\dot{\mathbf{x}}_{dI} = &\frac{-1}{\sqrt{\mathbf{h}_I^T\langle\!\langle \mathbf{e}_z\rangle\!\rangle\langle\!\langle \mathbf{z}_{dI}\rangle\!\rangle^2\langle\!\langle \mathbf{e}_z\rangle\!\rangle \mathbf{h}_I}}\left(\langle\!\langle \dot{\mathbf{z}}_{dI}\rangle\!\rangle\langle\!\langle \mathbf{e}_z\rangle\!\rangle \mathbf{h}_I + \langle\!\langle \mathbf{z}_{dI}\rangle\!\rangle\langle\!\langle \mathbf{e}_z\rangle\!\rangle \dot{\mathbf{h}}_I\right) + \left(\mathbf{h}_I^T\langle\!\langle \mathbf{e}_z\rangle\!\rangle\langle\!\langle \mathbf{z}_{dI}\rangle\!\rangle^2\langle\!\langle \mathbf{e}_z\rangle\!\rangle \mathbf{h}_I\right)^{-\frac{3}{2}}\\ &\cdot\left(\mathbf{h}_I^T\langle\!\langle \mathbf{e}_z\rangle\!\rangle\langle\!\langle \mathbf{z}_{dI}\rangle\!\rangle^2\langle\!\langle \mathbf{e}_z\rangle\!\rangle \dot{\mathbf{h}}_I + \mathbf{h}_I^T\langle\!\langle \mathbf{e}_z\rangle\!\rangle\langle\!\langle \mathbf{z}_{dI}\rangle\!\rangle\langle\!\langle \dot{\mathbf{z}}_{dI}\rangle\!\rangle\langle\!\langle \mathbf{e}_z\rangle\!\rangle \mathbf{h}_I\right)\cdot\langle\!\langle \mathbf{z}_{dI}\rangle\!\rangle\langle\!\langle \mathbf{e}_z\rangle\!\rangle \mathbf{h}_I\,,\end{aligned} \tag{10}$$

$$
\begin{aligned}
\ddot{\mathbf{x}}_{dI} = {} & \frac{-1}{\sqrt{\mathbf{h}_I^T\langle\langle\mathbf{e}_z\rangle\rangle\langle\langle\mathbf{z}_{dI}\rangle\rangle^2\langle\langle\mathbf{e}_z\rangle\rangle\mathbf{h}_I}}\left(\langle\langle\ddot{\mathbf{z}}_{dI}\rangle\rangle\langle\langle\mathbf{e}_z\rangle\rangle\mathbf{h}_I + 2\langle\langle\dot{\mathbf{z}}_{dI}\rangle\rangle\langle\langle\mathbf{e}_z\rangle\rangle\dot{\mathbf{h}}_I + \langle\langle\mathbf{z}_{dI}\rangle\rangle\langle\langle\mathbf{e}_z\rangle\rangle\ddot{\mathbf{h}}_I\right) \\
& - 3\left(\mathbf{h}_I^T\langle\langle\mathbf{e}_z\rangle\rangle\langle\langle\mathbf{z}_{dI}\rangle\rangle^2\langle\langle\mathbf{e}_z\rangle\rangle\mathbf{h}_I\right)^{-\frac{5}{2}}\left(\mathbf{h}_I^T\langle\langle\mathbf{e}_z\rangle\rangle\langle\langle\mathbf{z}_{dI}\rangle\rangle^2\langle\langle\mathbf{e}_z\rangle\rangle\dot{\mathbf{h}}_I + \mathbf{h}_I^T\langle\langle\mathbf{e}_z\rangle\rangle\langle\langle\mathbf{z}_{dI}\rangle\rangle\langle\langle\dot{\mathbf{z}}_{dI}\rangle\rangle\langle\langle\mathbf{e}_z\rangle\rangle\mathbf{h}_I\right)^2 \\
& \cdot\langle\langle\mathbf{z}_{dI}\rangle\rangle\langle\langle\mathbf{e}_z\rangle\rangle\mathbf{h}_I + \left(\mathbf{h}_I^T\langle\langle\mathbf{e}_z\rangle\rangle\langle\langle\mathbf{z}_{dI}\rangle\rangle^2\langle\langle\mathbf{e}_z\rangle\rangle\mathbf{h}_I\right)^{-\frac{3}{2}}\Big[\Big(\dot{\mathbf{h}}_I^T\langle\langle\mathbf{e}_z\rangle\rangle\langle\langle\mathbf{z}_{dI}\rangle\rangle^2\langle\langle\mathbf{e}_z\rangle\rangle\dot{\mathbf{h}}_I \\
& + 2\mathbf{h}_I^T\langle\langle\mathbf{e}_z\rangle\rangle\langle\langle\dot{\mathbf{z}}_{dI}\rangle\rangle\langle\langle\mathbf{z}_{dI}\rangle\rangle\langle\langle\mathbf{e}_z\rangle\rangle\dot{\mathbf{h}}_I + 2\mathbf{h}_I^T\langle\langle\mathbf{e}_z\rangle\rangle\langle\langle\mathbf{z}_{dI}\rangle\rangle\langle\langle\dot{\mathbf{z}}_{dI}\rangle\rangle\langle\langle\mathbf{e}_z\rangle\rangle\dot{\mathbf{h}}_I + \mathbf{h}_I^T\langle\langle\mathbf{e}_z\rangle\rangle\langle\langle\mathbf{z}_{dI}\rangle\rangle^2\langle\langle\mathbf{e}_z\rangle\rangle\ddot{\mathbf{h}}_I \\
& + \mathbf{h}_I^T\langle\langle\mathbf{e}_z\rangle\rangle\langle\langle\dot{\mathbf{z}}_{dI}\rangle\rangle^2\langle\langle\mathbf{e}_z\rangle\rangle\mathbf{h}_I + \mathbf{h}_I^T\langle\langle\mathbf{e}_z\rangle\rangle\langle\langle\mathbf{z}_{dI}\rangle\rangle\langle\langle\ddot{\mathbf{z}}_{dI}\rangle\rangle\langle\langle\mathbf{e}_z\rangle\rangle\mathbf{h}_I\Big)\cdot\langle\langle\mathbf{z}_{dI}\rangle\rangle\langle\langle\mathbf{e}_z\rangle\rangle\mathbf{h}_I \\
& + 2\left(\mathbf{h}_I^T\langle\langle\mathbf{e}_z\rangle\rangle\langle\langle\mathbf{z}_{dI}\rangle\rangle^2\langle\langle\mathbf{e}_z\rangle\rangle\dot{\mathbf{h}}_I + \mathbf{h}_I^T\langle\langle\mathbf{e}_z\rangle\rangle\langle\langle\mathbf{z}_{dI}\rangle\rangle\langle\langle\dot{\mathbf{z}}_{dI}\rangle\rangle\langle\langle\mathbf{e}_z\rangle\rangle\mathbf{h}_I\right)\cdot\left(\langle\langle\dot{\mathbf{z}}_{dI}\rangle\rangle\langle\langle\mathbf{e}_z\rangle\rangle\mathbf{h}_I + \langle\langle\mathbf{z}_{dI}\rangle\rangle\langle\langle\mathbf{e}_z\rangle\rangle\dot{\mathbf{h}}_I\right)\Big].
\end{aligned}
\tag{11}
$$

5 Attitude Tracking Dynamics

In terms of the error rotation matrix $\mathbf{R}_{BD} = \begin{bmatrix}\mathbf{x}_{dB} & \mathbf{y}_{dB} & \mathbf{z}_{dB}\end{bmatrix}$ the attitude kinematic equation is simply

$$
\dot{\mathbf{R}}_{BD} = -\langle\langle\boldsymbol{\omega}_B^{DB}\rangle\rangle\mathbf{R}_{BD}\ , \tag{12}
$$

where $\boldsymbol{\omega}_B^{DB}$ is the relative angular velocity between the body-fixed frame B and the desired frame D given in B. Sometimes it is more convenient to write $\mathbf{R}_{BD}$ as a vector. We define $\vec{\mathbf{R}}_{BD} = \begin{bmatrix}\mathbf{x}_{dB}^T & \mathbf{y}_{dB}^T & \mathbf{z}_{dB}^T\end{bmatrix}^T$ and accordingly

$$
\dot{\vec{\mathbf{R}}}_{BD} = \begin{bmatrix}-\langle\langle\boldsymbol{\omega}_B^{DB}\rangle\rangle\mathbf{x}_{dB}\\ -\langle\langle\boldsymbol{\omega}_B^{DB}\rangle\rangle\mathbf{y}_{dB}\\ -\langle\langle\boldsymbol{\omega}_B^{DB}\rangle\rangle\mathbf{z}_{dB}\end{bmatrix} = \begin{bmatrix}\langle\langle\mathbf{x}_{dB}\rangle\rangle\boldsymbol{\omega}_B^{DB}\\ \langle\langle\mathbf{y}_{dB}\rangle\rangle\boldsymbol{\omega}_B^{DB}\\ \langle\langle\mathbf{z}_{dB}\rangle\rangle\boldsymbol{\omega}_B^{DB}\end{bmatrix} = \begin{bmatrix}\langle\langle\mathbf{x}_{dB}\rangle\rangle\\ \langle\langle\mathbf{y}_{dB}\rangle\rangle\\ \langle\langle\mathbf{z}_{dB}\rangle\rangle\end{bmatrix}\boldsymbol{\omega}_B^{DB} = \langle\langle\vec{\mathbf{R}}_{BD}\rangle\rangle\boldsymbol{\omega}_B^{DB}\ , \tag{13}
$$

where, with a slight abuse of notation, we define $\langle\langle\vec{\mathbf{R}}_{BD}\rangle\rangle := \begin{bmatrix}\langle\langle\mathbf{x}_{dB}\rangle\rangle^T & \langle\langle\mathbf{y}_{dB}\rangle\rangle^T & \langle\langle\mathbf{z}_{dB}\rangle\rangle^T\end{bmatrix}^T$. By comparison of (12) with

$$
\begin{aligned}
\dot{\mathbf{R}}_{BD} &= \dot{\mathbf{R}}_{BI}\mathbf{R}_{ID} + \mathbf{R}_{BI}\dot{\mathbf{R}}_{ID} = -\langle\langle\boldsymbol{\omega}_B^{IB}\rangle\rangle\mathbf{R}_{BI}\mathbf{R}_{ID} + \mathbf{R}_{BI}\dot{\mathbf{R}}_{ID}\mathbf{R}_{ID}^T\mathbf{R}_{BI}^T\mathbf{R}_{BI}\mathbf{R}_{ID} \\
&= -\langle\langle\boldsymbol{\omega}_B^{IB}\rangle\rangle\mathbf{R}_{BD} + \mathbf{R}_{BI}\dot{\mathbf{R}}_{ID}\mathbf{R}_{ID}^T\mathbf{R}_{BI}^T\mathbf{R}_{BD} = -\left(\langle\langle\boldsymbol{\omega}_B^{IB}\rangle\rangle - \mathbf{R}_{BI}\dot{\mathbf{R}}_{ID}\mathbf{R}_{ID}^T\mathbf{R}_{BI}^T\right)\mathbf{R}_{BD}
\end{aligned}
\tag{14}
$$

we recognize that

$$
\boldsymbol{\omega}_B^{DB} = \rangle\rangle\langle\langle\boldsymbol{\omega}_B^{IB}\rangle\rangle - \mathbf{R}_{BI}\dot{\mathbf{R}}_{ID}\mathbf{R}_{ID}^T\mathbf{R}_{BI}^T\langle\langle = \rangle\rangle\langle\langle\boldsymbol{\omega}_B^{IB}\rangle\rangle - \langle\langle\boldsymbol{\omega}_B^{ID}\rangle\rangle\langle\langle \tag{15}
$$

holds. Note that all quantities appearing in (15) are known command signals or assumed to be accessible.

To derive the attitude error kinematics with respect to $\mathbf{z}_{dB}$ and $\mathbf{x}_{dAxy}$ we first notice that the time derivative of $\mathbf{z}_{dB} = \mathbf{R}_{BD}\mathbf{e}_z$ is obviously given by the last three entries of (13) which read

$$
\dot{\mathbf{z}}_{dB} = -\langle\langle\boldsymbol{\omega}_B^{DB}\rangle\rangle\mathbf{z}_{dB} = \langle\langle\mathbf{z}_{dB}\rangle\rangle\boldsymbol{\omega}_B^{DB}\ . \tag{16}
$$

The dynamics of $\mathbf{x}_{dAxy}$ are given by the first two rows of the dynamics of $\mathbf{x}_{dA} = \mathbf{R}_{AD}\mathbf{e}_x = \mathbf{R}_{AB}\mathbf{R}_{BD}\mathbf{e}_x$. Deriving the preceding expression with respect to time yields

$$
\begin{aligned}
\dot{\mathbf{x}}_{dA} &= \dot{\mathbf{R}}_{AB}\mathbf{R}_{BD}\mathbf{e}_x + \mathbf{R}_{AB}\dot{\mathbf{R}}_{BD}\mathbf{e}_x = \dot{\mathbf{R}}_{AB}\mathbf{R}_{BA}\mathbf{R}_{AD}\mathbf{e}_x + \mathbf{R}_{AB}\left(-\langle\langle\boldsymbol{\omega}_B^{DB}\rangle\rangle\right)\mathbf{R}_{BA}\mathbf{R}_{AD}\mathbf{e}_x \\
&= \dot{\mathbf{R}}_{AB}\mathbf{R}_{AB}^T\mathbf{x}_{dA} - \mathbf{R}_{AB}\langle\langle\boldsymbol{\omega}_B^{DB}\rangle\rangle\mathbf{R}_{AB}^T\mathbf{x}_{dA} = \left(\dot{\mathbf{R}}_{AB}\mathbf{R}_{AB}^T - \mathbf{R}_{AB}\langle\langle\boldsymbol{\omega}_B^{DB}\rangle\rangle\mathbf{R}_{AB}^T\right)\mathbf{x}_{dA}\ .
\end{aligned}
\tag{17}
$$

Using (4) and $\dot{\mathbf{R}}_{AB} = -\langle\langle\boldsymbol{\omega}_A^{BA}\rangle\rangle\mathbf{R}_{AB}$ the expression in brackets can be rewritten as

$$
\dot{\mathbf{R}}_{AB}\mathbf{R}_{AB}^T - \mathbf{R}_{AB}\langle\langle\boldsymbol{\omega}_B^{DB}\rangle\rangle\mathbf{R}_{AB}^T = -\langle\langle\boldsymbol{\omega}_A^{BA}\rangle\rangle - \langle\langle\boldsymbol{\omega}_A^{DB}\rangle\rangle = -\langle\langle\boldsymbol{\omega}_A^{DA}\rangle\rangle \tag{18}
$$

and hence

$$\dot{\mathbf{x}}_{dA} = -\langle\!\langle \boldsymbol{\omega}_A^{DA} \rangle\!\rangle \mathbf{x}_{dA} = \langle\!\langle \mathbf{x}_{dA} \rangle\!\rangle \boldsymbol{\omega}_A^{DA} \,. \tag{19}$$

Since the relative rotation of the frames A and D occurs only about their common z-axis it holds that $\boldsymbol{\omega}_A^{DA} = \begin{bmatrix} 0 & 0 & \omega_{Az}^{DA} \end{bmatrix}^T$ and thus

$$\dot{\mathbf{R}}_{AB}\mathbf{R}_{AB}^T - \mathbf{R}_{AB}\langle\!\langle \boldsymbol{\omega}_B^{DB} \rangle\!\rangle \mathbf{R}_{AB}^T = -\langle\!\langle \boldsymbol{\omega}_A^{DA} \rangle\!\rangle = \begin{bmatrix} 0 & \omega_{Az}^{DA} & 0 \\ -\omega_{Az}^{DA} & 0 & 0 \\ 0 & 0 & 0 \end{bmatrix} . \tag{20}$$

The expression on the left hand side of (20) is a function of $\mathbf{z}_{dB}$ and $\boldsymbol{\omega}_B^{DB}$. To see this, we first express the rotation matrix $\mathbf{R}_{AB}$ by $\mathbf{z}_{dB}$. According to Euler's formula (see e.g. [15]), which indicates the rotation matrix in terms of axis and angle, it holds that

$$\mathbf{R}_{AB} = \cos(\varphi)\mathbf{I}_3 + (1 - \cos(\varphi))\mathbf{e}_\varphi \mathbf{e}_\varphi^T - \sin(\varphi)\langle\!\langle \mathbf{e}_\varphi \rangle\!\rangle \,. \tag{21}$$

Using (8), the unit length of $\mathbf{z}_{dB}$ and noting that $\cos(\varphi) = z_{dBz}$ and $\sin(\varphi)\mathbf{e}_\varphi = \langle\!\langle \mathbf{e}_z \rangle\!\rangle \mathbf{z}_{dB}$ one obtains

$$\begin{aligned} \mathbf{R}_{AB} &= z_{dBz}\mathbf{I}_3 + \frac{(1 - z_{dBz})}{(1 - z_{dBz}^2)} \begin{bmatrix} -z_{dBy} \\ z_{dBx} \\ 0 \end{bmatrix} \begin{bmatrix} -z_{dBy} & z_{dBx} & 0 \end{bmatrix} - \langle\!\langle \langle\!\langle \mathbf{e}_z \rangle\!\rangle \mathbf{z}_{dB} \rangle\!\rangle \\ &= \begin{bmatrix} 1 - \frac{z_{dBx}^2}{1+z_{dBz}} & \frac{-z_{dBx}z_{dBy}}{1+z_{dBz}} & -z_{dBx} \\ \frac{-z_{dBx}z_{dBy}}{1+z_{dBz}} & 1 - \frac{z_{dBy}^2}{1+z_{dBz}} & -z_{dBy} \\ z_{dBx} & z_{dBy} & z_{dBz} \end{bmatrix} . \end{aligned} \tag{22}$$

With the preceding equation and (16) one can evaluate the left hand side of (20) and identify

$$\omega_{Az}^{DA} = \begin{bmatrix} \frac{z_{dBx}}{1+z_{dBz}} & \frac{z_{dBy}}{1+z_{dBz}} & 1 \end{bmatrix} \boldsymbol{\omega}_B^{DB} \,. \tag{23}$$

Inserting (23) into (19) and evaluating the first and second row finally yields

$$\dot{\mathbf{x}}_{dAxy} = \begin{bmatrix} x_{dAy} \\ -x_{dAx} \end{bmatrix} \omega_{Az}^{DA} = \begin{bmatrix} x_{dAy} \\ -x_{dAx} \end{bmatrix} \begin{bmatrix} \frac{z_{dBx}}{1+z_{dBz}} & \frac{z_{dBy}}{1+z_{dBz}} & 1 \end{bmatrix} \boldsymbol{\omega}_B^{DB} \,. \tag{24}$$

Defining the unit vector

$$\mathbf{e}_\perp = \frac{1}{\sqrt{z_{dBx}^2 + z_{dBy}^2}} \begin{bmatrix} z_{dBx} \\ z_{dBy} \\ 0 \end{bmatrix} \tag{25}$$

one can reformulate (24) to obtain

$$\dot{\mathbf{x}}_{dAxy} = \begin{bmatrix} x_{dAy} \\ -x_{dAx} \end{bmatrix} \left(\frac{\sqrt{z_{dBx}^2 + z_{dBy}^2}}{1 + z_{dBz}} \mathbf{e}_\perp^T + \mathbf{e}_z^T \right) \boldsymbol{\omega}_B^{DB} \,. \tag{26}$$

Finally, the dynamics of $\boldsymbol{\omega}_B^{DB}$ complete the attitude tracking dynamics. Using (6), the derivative of $\boldsymbol{\omega}_B^{DB}$ with respect to time is identified as

$$\dot{\boldsymbol{\omega}}_B^{DB} = \dot{\boldsymbol{\omega}}_B^{IB} - \dot{\boldsymbol{\omega}}_B^{ID} = \mathbf{J}^{-1}\left(-\langle\!\langle \boldsymbol{\omega}_B^{IB} \rangle\!\rangle \mathbf{J}\boldsymbol{\omega}_B^{IB} + \boldsymbol{\tau} \right) - \dot{\boldsymbol{\omega}}_B^{ID} \,, \tag{27}$$

where $\dot{\boldsymbol{\omega}}_B^{ID}$ is obtained by deriving the expression $\boldsymbol{\omega}_B^{ID} = \rangle\!\rangle \mathbf{R}_{BI}\dot{\mathbf{R}}_{ID}\mathbf{R}_{ID}^T\mathbf{R}_{BI}^T \langle\!\langle$ introduced in (15) with respect to time, which yields

$$\begin{aligned} \dot{\boldsymbol{\omega}}_B^{ID} = \rangle\!\rangle &- \langle\!\langle \boldsymbol{\omega}_B^{IB} \rangle\!\rangle \mathbf{R}_{BI}\dot{\mathbf{R}}_{ID}\mathbf{R}_{ID}^T\mathbf{R}_{BI}^T + \mathbf{R}_{BI}\ddot{\mathbf{R}}_{ID}\mathbf{R}_{ID}^T\mathbf{R}_{BI}^T + \mathbf{R}_{BI}\dot{\mathbf{R}}_{ID}\dot{\mathbf{R}}_{ID}^T\mathbf{R}_{BI}^T \\ &+ \mathbf{R}_{BI}\dot{\mathbf{R}}_{ID}\mathbf{R}_{ID}^T\mathbf{R}_{BI}^T \langle\!\langle \boldsymbol{\omega}_B^{IB} \rangle\!\rangle \langle\!\langle \,. \end{aligned} \tag{28}$$

Together with (12), equation (27) forms the open loop dynamics with the corresponding state $\mathbf{W} = (\mathbf{R}_{BD}, \boldsymbol{\omega}_B^{DB}) \in \mathcal{W} = SO(3) \times \mathbb{R}^3$. Alternatively, the open loop dynamics can be expressed locally (but almost globally) by (16), (24) and (27) with the corresponding state $\mathfrak{w} = \begin{bmatrix} \mathbf{z}_{dB}^T & \mathbf{x}_{dAxy}^T & (\boldsymbol{\omega}_B^{DB})^T \end{bmatrix}^T \in \mathcal{S}^2 \times \mathcal{S} \times \mathbb{R}^3$. This fact is analyzed in the following remark.

Remark 1. The heading state $\mathbf{x}_{dAxy}$ is not defined if $\mathbf{z}_{dB} = -\mathbf{e}_z \Leftrightarrow \varphi = \pi$, meaning that the current thrust direction is pointing in the opposite direction of the desired one. Considering that $\mathbf{x}_{dA} = \mathbf{R}_{AB}\mathbf{R}_{BD}\mathbf{e}_x$, this can be recognized by the fact that $\mathbf{R}_{AB}$ in (22) has a singularity in that case. Clearly, the error rotation matrix $\mathbf{R}_{BD}$ as the natural attitude error state is well defined everywhere and accordingly also $\mathbf{z}_{dB}$, which is the last column of $\mathbf{R}_{BD}$, is not subject to any singularities.

As a consequence of $\mathbf{x}_{dAxy}$ being not defined if $\mathbf{z}_{dB} = -\mathbf{e}_z$ we formulate the following standing assumption that enables us to globally consider the control law developed in the following as both a function of $\mathbf{W}$ and a function of $\mathfrak{w}$.

Assumption 1 (Standing Assumption)**.** Any expression appearing in the control law, defining the control torque $\boldsymbol{\tau}$, is constructed such that it depends only on $\mathbf{z}_{dB}$ and $\boldsymbol{\omega}_B^{DB}$ if $\mathbf{z}_{dB} = -\mathbf{e}_z \Leftrightarrow \varphi = \pi$. As a consequence we can globally write $\boldsymbol{\tau}(\mathbf{W})$ as well as $\boldsymbol{\tau}(\mathfrak{w})$.

Remark 2. As can be easily verified, the unit vectors $\mathbf{e}_\perp$, $\mathbf{e}_\varphi$ and $\mathbf{e}_z$ define an orthonormal basis $\{\mathbf{e}_\perp, \mathbf{e}_\varphi, \mathbf{e}_z\}$. This fact will be extensively used in Subsection 6.2, where the damping of the closed loop is designed.

6 Controller Design

In this section, we will first execute an input transformation, such that the controller presented in [8] could be applied without any changes. We will also motivate the basic idea of the controller design before we restate it using the new attitude parametrization. Moreover, we apply some minor changes to the potential energy, which significantly facilitate the local analysis of the equilibrium points.

Inserting the input transformation

$$\boldsymbol{\tau} = k(\mathbf{W})\langle\!\langle \boldsymbol{\omega}_B^{IB} \rangle\!\rangle \mathbf{J}\boldsymbol{\omega}_B^{IB} - (k(\mathbf{W}) - 1)\left(\langle\!\langle \boldsymbol{\omega}_B^{ID} \rangle\!\rangle \mathbf{J}(\boldsymbol{\omega}_B^{IB} - \boldsymbol{\omega}_B^{ID}) + \langle\!\langle \boldsymbol{\omega}_B^{IB} \rangle\!\rangle \mathbf{J}\boldsymbol{\omega}_B^{ID}\right) + \mathbf{J}\dot{\boldsymbol{\omega}}_B^{ID} + \tilde{\boldsymbol{\tau}}\,, \quad (29)$$

which consists of both the new control input $\tilde{\boldsymbol{\tau}}$ and suitable feedforward terms, into (27) yields

$$\dot{\boldsymbol{\omega}}_B^{DB} = \mathbf{J}^{-1}\left((k(\mathbf{W}) - 1)\langle\!\langle \boldsymbol{\omega}_B^{DB} \rangle\!\rangle \mathbf{J}\boldsymbol{\omega}_B^{DB} + \tilde{\boldsymbol{\tau}}\right)\,. \quad (30)$$

Therein, $k(\mathbf{W})$ can be any locally Lipschitz continuous function on $\mathcal{W}$ satisfying Assumption 1. However, in order to facilitate the local stability analysis in Section 7.1, we will restrict us to functions, which can be globally written as $k(\mathbf{z}_{dB}, \boldsymbol{\omega}_B^{DB})$. For the sake of convenience, k is often chosen constant. For example $k = 1$ will cancel the coriolis term, whereas $k = 0$ yields $\boldsymbol{\tau} = \tilde{\boldsymbol{\tau}}$ in the case of a setpoint control (when $\mathbf{R}_{ID}$ is constant). It will turn out that the stability properties of the closed loop do not depend on the particular choice of k. Together with (12) or alternatively (16) and (24) the preceding equation forms the new open loop dynamics. For the convenience of the reader the respective equations are assembled in the following. Using the global state representation $\mathbf{W}$ one obtains the open loop system

$$\dot{\mathbf{R}}_{BD} = -\langle\!\langle \boldsymbol{\omega}_B^{DB} \rangle\!\rangle \mathbf{R}_{BD}\,, \quad (31)$$

$$\dot{\boldsymbol{\omega}}_B^{DB} = \mathbf{J}^{-1}\left((k(\mathbf{z}_{dB}, \boldsymbol{\omega}_B^{DB}) - 1)\langle\!\langle \boldsymbol{\omega}_B^{DB} \rangle\!\rangle \mathbf{J}\boldsymbol{\omega}_B^{DB} + \tilde{\boldsymbol{\tau}}\right)\,, \quad (32)$$

whereas using $\mathfrak{w}$ as the state representation of choice leads to

$$\dot{\mathbf{z}}_{dB} = \langle\!\langle \mathbf{z}_{dB} \rangle\!\rangle \boldsymbol{\omega}_B^{DB} , \tag{33}$$

$$\dot{\mathbf{x}}_{dAxy} = \begin{bmatrix} x_{dAy} \\ -x_{dAx} \end{bmatrix} \begin{bmatrix} \frac{z_{dBx}}{1+z_{dBz}} & \frac{z_{dBy}}{1+z_{dBz}} & 1 \end{bmatrix} \boldsymbol{\omega}_B^{DB} , \tag{34}$$

$$\dot{\boldsymbol{\omega}}_B^{DB} = \mathbf{J}^{-1} \left((k(\mathbf{z}_{dB}, \boldsymbol{\omega}_B^{DB}) - 1) \langle\!\langle \boldsymbol{\omega}_B^{DB} \rangle\!\rangle \mathbf{J} \boldsymbol{\omega}_B^{DB} + \tilde{\boldsymbol{\tau}} \right) . \tag{35}$$

The control law presented in [8] could now be directly applied to $\tilde{\boldsymbol{\tau}}$ and would achieve asymptotic attitude tracking. In the following some slight modifications to that control law will be introduced, but we adopt the input constraint

$$\|\tilde{\boldsymbol{\tau}}_{xy}\| \leq \bar{\tau}_{xy} , \quad |\tilde{\tau}_z| \leq \bar{\tau}_z , \tag{36}$$

where $\bar{\tau}_{xy}$ and $\bar{\tau}_z$ are positive constants and $\bar{\tau}_{xy} \gg \bar{\tau}_z$ holds. Although $\tilde{\boldsymbol{\tau}}$ is not the actual control torque, we nevertheless consider the constraint, since, as mentioned above, $\tilde{\boldsymbol{\tau}}$ equals $\boldsymbol{\tau}$ if k is chosen to be zero and a setpoint control is considered. Moreover, the constraint can be easily dropped if desired. Due to the similarity of (30) and (6), we will sloppily refer to $\tilde{\boldsymbol{\tau}}$ as the control torque from time to time, although it is clear that the actual torque is $\boldsymbol{\tau}$.

The controller design is based on an energy shaping approach as presented e.g. in [14]. The control law is constructed such that the closed loop system is described by means of an assigned continuously differentiable energy function V, which has a strict minimum at the desired equilibrium point $\mathbf{W}_d = (\mathbf{I}_3, \mathbf{0}) \Leftrightarrow \mathfrak{w}_d = \begin{bmatrix} \mathbf{e}_z^T & \begin{bmatrix} 1 & 0 \end{bmatrix} & \mathbf{0}^T \end{bmatrix}^T$. In the following we will assign an energy function

$$V(\mathbf{W}) = E_{rot}(\boldsymbol{\omega}_B^{DB}) + E_{pot}(\mathbf{R}_{BD}) = \frac{1}{2} (\boldsymbol{\omega}_B^{DB})^T \mathbf{J} \boldsymbol{\omega}_B^{DB} + E_{pot}(\mathbf{R}_{BD}) , \tag{37}$$

which is composed of a kinetic and a potential energy part and fulfills $V(\mathbf{W}_d) = 0$ and $V(\mathbf{W}) > 0$ if $\mathbf{W} \neq \mathbf{W}_d$. Moreover, since E_{rot} is a radially unbounded function and the attitude space is compact, it holds that all sublevel sets of V are compact and include $\mathbf{W}_d$. Taking the derivative of V with respect to time yields

$$\dot{V}(\mathbf{W}) = (\boldsymbol{\omega}_B^{DB})^T \mathbf{J} \dot{\boldsymbol{\omega}}_B^{DB} + \frac{\partial E_{pot}}{\partial \vec{\mathbf{R}}_{BD}} \dot{\vec{\mathbf{R}}}_{BD} = (\boldsymbol{\omega}_B^{DB})^T \tilde{\boldsymbol{\tau}} + \underbrace{\frac{\partial E_{pot}}{\partial \vec{\mathbf{R}}_{BD}} \langle\!\langle \vec{\mathbf{R}}_{BD} \rangle\!\rangle}_{-\mathbf{T}^T(\mathbf{R}_{BD})} \boldsymbol{\omega}_B^{DB} , \tag{38}$$

where $\mathbf{T}$ can be identified as the torque field resulting from the potential energy E_{pot}. Now, by choosing the control law

$$\tilde{\boldsymbol{\tau}} = \mathbf{T}(\mathbf{R}_{BD}) - \mathbf{D}(\mathbf{W}) \boldsymbol{\omega}_B^{DB} , \tag{39}$$

where $\mathbf{D}(\mathbf{W}) \geq \mathbf{0}$ is a state dependent damping matrix, and inserting it into (38), one obtains

$$\dot{V}(\mathbf{W}) = -(\boldsymbol{\omega}_B^{DB})^T \mathbf{D}(\mathbf{W}) \boldsymbol{\omega}_B^{DB} \leq \mathbf{0} . \tag{40}$$

It follows from (40) that the sublevel sets of V are not only compact but also positively invariant, which proves global stability of the desired equilibrium. After explicitly defining the control law (39) in the next subsections, further stability properties are analyzed in Section 7.

6.1 Shaping of the Potential Energy

We will now state the potential energy which is assigned to the closed loop system. Apart from some minor modifications discussed at the end of this subsection, it is largely identical to the one given in [8]. The potential energy E_{pot} necessarily needs to depend on appropriate error functions characterizing the thrust direction error and the heading error. A natural error function indicating the alignment error of the thrust is the angle $\varphi = \arccos(z_{dBz})$ whereas the angle $\vartheta = \arccos(x_{dAx})$ can be considered a measure for the heading error. We propose a potential energy of the form $E_{pot}(\varphi, \vartheta)$. To be an appropriate energy function, $E_{pot}(\varphi, \vartheta)$ has to be continuously differentiable on the domain $[0,\pi]\times[0,\pi]$ with its only minimum at $(\varphi, \vartheta) = (0,0)$ and we moreover claim

$$\frac{\partial E_{pot}}{\partial \vartheta}(\pi, \vartheta) = 0 \qquad \forall \vartheta \,, \tag{41}$$

$$\frac{\partial E_{pot}}{\partial \vartheta}(0, \vartheta) > 0 \qquad \text{if } \vartheta \in \,]0,\pi[\,, \tag{42}$$

$$\frac{\partial E_{pot}}{\partial \varphi}(\varphi, \vartheta) > 0 \qquad \text{if } (\varphi, \vartheta) \in \,]0,\pi[\times[0,\pi]\,, \tag{43}$$

$$\frac{\partial E_{pot}}{\partial \varphi}(\varphi, \vartheta) = 0 \qquad \text{if } (\varphi, \vartheta) \in \{0,\pi\}\times[0,\pi]\,, \tag{44}$$

$$\frac{\partial E_{pot}}{\partial \vartheta}(\varphi, \vartheta) = 0 \qquad \text{if } (\varphi, \vartheta) \in [0,\pi]\times\{0,\pi\}\,. \tag{45}$$

The first constraint guarantees that $\mathbf{T}$ is compliant with Assumption 1 by ensuring that $E_{pot}(\varphi, \vartheta)$ does not depend on ϑ if $\varphi = \pi$. As analyzed in Remark 1 this is necessary since ϑ as a function of $\mathbf{x}_{dAxy}$, which is not unique in this case. The second constraint assures that the potential energy is increasing with a growing heading error at least at $\varphi = 0$ (and due to the differentiability also in a neighborhood of $\varphi = 0$). The third constraint claims that the same is true with respect to the thrust direction error but independently of the heading error. Finally, the fourth and fifth constraint serves to guarantee a continuous torque field $\mathbf{T}$ over the whole state space $\mathcal{W}$. Alltogether, the constraints imply that first, all critical points of E_{pot} are given by the set $(\varphi, \vartheta) \in \{(0,0) \cup (0,\pi) \cup \{\pi\}\times[0,\pi]\}$ and second, E_{pot} is maximal for $(\varphi, \vartheta) \in \{\{\pi\}\times[0,\pi]\}$. It is clear from physical insight that the set of critical points of the potential energy defines the state space region where the torque field disappears and thus it also defines the set of equilibrium points of the closed loop system. It was shown in [1] that due to the topological structure of the attitude space further equilibrium points besides the desired one must exist if a continuous control law is applied. In detail we choose a potential energy function

$$E_{pot}(\varphi, \vartheta) = E_{\varphi}(\varphi) + E_{\vartheta}(\varphi, \vartheta)\,, \tag{46}$$

where

$$E_{\varphi}(\varphi) = c_{\varphi}\int_0^{\varphi} \Lambda_{\varphi_l}^{\varphi_u}(\zeta)\, d\zeta\,, \quad E_{\vartheta}(\varphi, \vartheta) = \begin{cases} \frac{\left(\cos(\frac{\varphi}{2}) - \cos(\frac{\varphi_u}{2})\right)^2}{\left(1-\cos(\frac{\varphi_u}{2})\right)^2} c_{\vartheta}\int_0^{\vartheta} \Lambda_{\vartheta_l}^{\vartheta_u}(\zeta)\, d\zeta & \text{if } \varphi \le \varphi_u \\ 0 & \text{if } \varphi > \varphi_u \end{cases} \tag{47}$$

and c_{φ}, c_{ϑ} are positive constants. The structure of the energy components chosen in (47) immediately guarantees compliance with the constraints (41), (42), (44) and (45). To guarantee (43) a suitable parameter set (c_{φ}, c_{ϑ}, φ_l, φ_u, ϑ_l, ϑ_u) has to be chosen, which is always possible. To see this, note that choosing c_{ϑ} sufficiently small will always lead to compliance with (43).

As in (38) one has to take the derivative of E_{pot} with respect to time to compute the torque field $\mathbf{T}$ that E_{pot} generates. It holds that

$$\dot{E}_{pot} = \frac{\partial E_{pot}}{\partial \varphi}\dot{\varphi} + \frac{\partial E_{pot}}{\partial \vartheta}\dot{\vartheta} = -\mathbf{T}^T \boldsymbol{\omega}_B^{DB}\,, \tag{48}$$

where

$$\dot{\varphi} = \frac{-\dot{z}_{dBz}}{\sqrt{1 - z_{dBz}^2}} = -\frac{1}{\sqrt{z_{dBx}^2 + z_{dBy}^2}} \begin{bmatrix} -z_{dBy} \\ z_{dBx} \\ 0 \end{bmatrix}^T \boldsymbol{\omega}_B^{DB} = -\mathbf{e}_\varphi^T \boldsymbol{\omega}_B^{DB} \tag{49}$$

is obtained using (16) and the unit length of $\mathbf{z}_{dB}$ and

$$\dot{\vartheta} = \frac{-\dot{x}_{dAx}}{\sqrt{1 - x_{dAx}^2}} = \frac{-x_{dAy}}{\sqrt{1 - x_{dAx}^2}} \left(\frac{\sqrt{z_{dBx}^2 + z_{dBy}^2}}{1 + z_{dBz}} \mathbf{e}_\perp^T + \mathbf{e}_z^T \right) \boldsymbol{\omega}_B^{DB} \tag{50}$$

is computed analogously using (26). Decomposing $\mathbf{T}$ into parts according to the energy components E_φ and E_ϑ from which they originate and according to their effective directions $\mathbf{e}_\varphi$, $\mathbf{e}_\perp$ and $\mathbf{e}_z$ results in

$$\mathbf{T} = \mathbf{T}_\varphi^\varphi + \mathbf{T}_\varphi^\vartheta + \mathbf{T}_\perp^\vartheta + \mathbf{T}_z^\vartheta , \tag{51}$$

where the superscript indicates the energy component and the subscript indicates the effective direction. Using (48), (49), (50) and (47) the components in (51) are identified as

$$\begin{aligned}
\mathbf{T}_\varphi^\varphi &= \frac{\partial E_\varphi}{\partial \varphi}\, \mathbf{e}_\varphi = \Lambda_{\varphi_l}^{\varphi_u}(\varphi)\mathbf{e}_\varphi , \\
\mathbf{T}_\varphi^\vartheta &= \frac{\partial E_\vartheta}{\partial \varphi}\, \mathbf{e}_\varphi = \\
&= \begin{cases} \frac{-\left(\cos(\frac{\varphi}{2}) - \cos(\frac{\varphi_u}{2})\right)\sin(\frac{\varphi}{2})}{\left(1-\cos(\frac{\varphi_u}{2})\right)^2} c_\vartheta \int_0^\vartheta \Lambda_{\vartheta_l}^{\vartheta_u}(\zeta)\, d\zeta\, \mathbf{e}_\varphi & \text{if } \varphi \le \varphi_u \\ \mathbf{0} & \text{if } \varphi > \varphi_u \end{cases} , \\
\mathbf{T}_\perp^\vartheta &= \frac{\partial E_\vartheta}{\partial \vartheta} \cdot \frac{x_{dAy}\sqrt{z_{dBx}^2 + z_{dBy}^2}}{\sqrt{1 - x_{dAx}^2}\,(1 + z_{dBz})}\, \mathbf{e}_\perp = \\
&= \begin{cases} \frac{\left(\cos(\frac{\varphi}{2}) - \cos(\frac{\varphi_u}{2})\right)^2}{\left(1-\cos(\frac{\varphi_u}{2})\right)^2} c_\vartheta \Lambda_{\vartheta_l}^{\vartheta_u}(\vartheta) \frac{x_{dAy}\sqrt{z_{dBx}^2+z_{dBy}^2}}{\sqrt{1-x_{dAx}^2}\,(1+z_{dBz})}\, \mathbf{e}_\perp & \text{if } \varphi \le \varphi_u \\ \mathbf{0} & \text{if } \varphi > \varphi_u \end{cases} , \\
\mathbf{T}_z^\vartheta &= \frac{\partial E_\vartheta}{\partial \vartheta} \cdot \frac{x_{dAy}}{\sqrt{1 - x_{dAx}^2}}\, \mathbf{e}_z = \\
&= \begin{cases} \frac{\left(\cos(\frac{\varphi}{2}) - \cos(\frac{\varphi_u}{2})\right)^2}{\left(1-\cos(\frac{\varphi_u}{2})\right)^2} c_\vartheta \Lambda_{\vartheta_l}^{\vartheta_u}(\vartheta) \frac{x_{dAy}}{\sqrt{1-x_{dAx}^2}}\, \mathbf{e}_z & \text{if } \varphi \le \varphi_u \\ \mathbf{0} & \text{if } \varphi > \varphi_u \end{cases} .
\end{aligned} \tag{52}$$

The chosen potential energy function (46) extends the potential energy E_φ, introduced in [7], by a further component E_ϑ. The energy E_φ can be thought of as the potential caused by a nonlinear saturating torsion spring arranged between the actual and the desired thrust direction. Accordingly, it generates a torque $\mathbf{T}_\varphi^\varphi$ depending only on φ, which ensures the alignment of the body-fixed z-axis. The energy component E_ϑ serves to generate control torques that reduce the heading error angle ϑ. Note that the φ-dependent prefactor in E_ϑ results in a decreasing influence of this energy component with an increasing thrust direction error φ. For $\varphi > \varphi_u$ it even disappears. Since large thrust direction errors can cause large deviations from the intended translational motion of the quadrotor, they indicate a critical situation. Thus, the behavior of E_ϑ is favorable since it forces the controller to prioritize the thrust alignment instead of reducing the heading error. In detail, the torques $\mathbf{T}_z^\vartheta$, $\mathbf{T}_\perp^\vartheta$ and $\mathbf{T}_\varphi^\vartheta$ are induced by E_ϑ. While $\mathbf{T}_z^\vartheta$ can be regarded as the "intended" torque, which, for a constant φ, acts around the z-axis analogous to $\mathbf{T}_\varphi^\varphi$, the components $\mathbf{T}_\perp^\vartheta$ and $\mathbf{T}_\varphi^\vartheta$ can be considered "parasitic". This is because $\mathbf{T}_\varphi^\vartheta$ always counteracts $\mathbf{T}_\varphi^\varphi$ and $\mathbf{T}_\perp^\vartheta$ induces a motion around $\mathbf{e}_\perp$, which does not contribute to a decrease of φ according to (49). At the same time, $\mathbf{T}_\perp^\vartheta$ reduces the available control authority for $\mathbf{T}_\varphi^\varphi$, since in view of (36)

$$\|\mathbf{T}_{xy}\| = \sqrt{(\|\mathbf{T}_\varphi^\varphi\| - \|\mathbf{T}_\varphi^\vartheta\|)^2 + \|\mathbf{T}_\perp^\vartheta\|^2} < \bar{\tau}_{xy} \tag{53}$$

must hold. Just like compliance with the constraint (43) (which in turn is equivalent to $\|\mathbf{T}_\varphi^\varphi\| - \|\mathbf{T}_\varphi^\vartheta\| > 0$) is a matter of parameterizing E_{pot}, the same holds for guaranteeing (53) and is always possible. Again, it can be verified that choosing c_ϑ sufficiently small will lead to compliance with (53). The second control input constraint given in (36) amounts to

$$|T_z| = \|\mathbf{T}_z^\vartheta\| < \bar{\tau}_z, \tag{54}$$

and is ensured by choosing $c_\vartheta < \frac{\bar{\tau}_z}{\sin(\vartheta_l)}$. Note that in contrast to (36) we have formulated (53) and (54) as strict inequalities in order to reserve some control torque for damping purposes.

In contrast to [8], the energy components E_φ and E_ϑ presented here were constructed using a slightly modified function $\Lambda_{\zeta_l}^{\zeta_u}(\zeta)$. Instead of a linear increasing and decreasing integrand, in (1) an integrand increasing and decreasing with the sine function is chosen. While the deviation from the linear function is negligible for reasonable values of φ_l, φ_u and ϑ_l, ϑ_u respectively, this choice significantly facilitates linearizing the closed loop system around its equilibrium points for the analysis of the local properties. Moreover, the φ-dependent prefactor in E_ϑ is different compared to [8]. Again, the main reason for the modification lies in the simplified local analysis, while not overly influencing the closed loop behavior.

6.2 Damping Injection

The damping matrix $\mathbf{D}$ needed to complete the control law (39) is adopted from [8] without changes and hence only adapted to the parametrization and the notation used. The basic idea is to decompose the angular velocity $\boldsymbol{\omega}_B^{DB}$ into components according to the orthonormal basis $\{\mathbf{e}_\perp, \mathbf{e}_\varphi, \mathbf{e}_z\}$ and to damp them individually. This is reasonable because they have a different meaning in view of the control task. The decomposition of $\boldsymbol{\omega}_B^{DB}$ reads

$$\boldsymbol{\omega}_B^{DB} = \mathbf{e}_\perp^T \boldsymbol{\omega}_B^{DB} \mathbf{e}_\perp + \mathbf{e}_\varphi^T \boldsymbol{\omega}_B^{DB} \mathbf{e}_\varphi + \mathbf{e}_z^T \boldsymbol{\omega}_B^{DB} \mathbf{e}_z = \omega_\perp \mathbf{e}_\perp + \omega_\varphi \mathbf{e}_\varphi + \omega_z \mathbf{e}_z \,. \tag{55}$$

Note that according to (49) it holds that $\omega_\varphi = -\dot{\varphi}$. By choosing a damping matrix of the form

$$\begin{aligned} \mathbf{D}(\mathbf{W}) &= \kappa_{xy}(\mathbf{W})\big(d_\varphi(\mathbf{W})\mathbf{e}_\varphi\mathbf{e}_\varphi^T + d_\perp \mathbf{e}_\perp \mathbf{e}_\perp^T\big) + \kappa_z(\mathbf{W}) d_z(\mathbf{W}) \mathbf{e}_z \mathbf{e}_z^T \\ &= \begin{bmatrix} \kappa_{xy}(\mathbf{W})\mathbf{D}_{xy}(\mathbf{W}) & \mathbf{0} \\ \mathbf{0} & \kappa_z(\mathbf{W}) d_z(\mathbf{W}) \end{bmatrix} \geq 0 \,, \end{aligned} \tag{56}$$

the damping coefficients d_φ, $d_\perp$ and d_z allow an individual damping of ω_φ, $\omega_\perp$ and ω_z. The submatrix $\mathbf{D}_{xy}$ in (56) reads

$$\mathbf{D}_{xy}(\mathbf{W}) = \frac{d_\varphi(\mathbf{W})}{z_{dBx}^2 + z_{dBy}^2} \begin{bmatrix} z_{dBy}^2 & -z_{dBx} z_{dBy} \\ -z_{dBx} z_{dBy} & z_{dBx}^2 \end{bmatrix} + \frac{d_\perp}{z_{dBx}^2 + z_{dBy}^2} \begin{bmatrix} z_{dBx}^2 & z_{dBx} z_{dBy} \\ z_{dBx} z_{dBy} & z_{dBy}^2 \end{bmatrix} \tag{57}$$

and the gains κ_{xy} and κ_z serve to saturate the damping torques if necessary. They are defined as

$$\kappa_{xy} = \min_{\kappa > 0, \left\|\mathbf{T}_{xy} - \kappa \cdot \mathbf{D}_{xy} \boldsymbol{\omega}_{Bxy}^{DB}\right\| = \bar{\tau}_{xy}} (1, \kappa) \,, \qquad \kappa_z = \min_{\kappa > 0, \left|T_z - \kappa \cdot d_z \omega_{Bz}^{DB}\right| = \bar{\tau}_z} (1, \kappa) \tag{58}$$

and guarantee compliance with (36). While the angular rate ω_z is about the thrust axis and hence does not at all influence the alignment of the thrust, this does not hold for $\omega_\perp$. In contrast, the angular rate $\omega_\perp$ indicates a motion around $\mathbf{e}_\perp$ causing the thrust vector to move perpendicular away from the shortest path to the desired thrust direction, which is given by a rotation around $\mathbf{e}_\varphi$. Consequently $\omega_\perp$ should always be damped and $d_\perp$ is chosen to be a positive constant. The choice of the damping coefficients d_φ and d_z given below, is guided by some simplifying considerations on the motion of the controlled system. These simplifications merely serve as tool for the design of d_φ and d_z and do not affect the stability analysis in Section 7.

Regarding the symmetry of a quadrotor, one can assume that $\mathbf{J} \approx \hat{\mathbf{J}} = \mathrm{diag}(\hat{J}_1, \hat{J}_1, \hat{J}_2) > \mathbf{0}$ approximately holds. Since moreover $\bar{\tau}_{xy} \gg \bar{\tau}_z$ and the primary objective is to align the thrust axis, one will usually construct the energies E_φ and E_ϑ such that the torque $\mathbf{T}^\varphi_\varphi$, which is designed to align the thrust, significantly dominates the other components $\mathbf{T}^\vartheta_\varphi$,$\mathbf{T}^\vartheta_\perp$ and $\mathbf{T}^\vartheta_z$. It is therefore plausible to assume that the control task is completed more or less sequentially. This means that first φ is driven to zero while ϑ remains more or less constant and only afterwards ϑ is reduced to zero. This implies that in the first phase the simplifying assumption $\boldsymbol{\omega}^{BD}_B \parallel \dot{\boldsymbol{\omega}}^{BD}_B \parallel \mathbf{e}_\varphi$ is justified and provided that $\kappa_{xy} = 1$, the scalar differential equation

$$\hat{J}_1 \ddot{\varphi} = -T_\varphi - d_\varphi(\mathbf{W}) \cdot \dot{\varphi} \quad \text{if } \varphi \neq 0\,,^1 \tag{59}$$

approximately holds, where $T_\varphi = \|\mathbf{T}^\varphi_\varphi\| - \|\mathbf{T}^\vartheta_\varphi\| > 0$. It can be seen from (52) that near $\varphi = 0$, where the small-angle approximation holds, the torque T_φ can be considered linear in φ. Reasonable values of φ_l are rather small and accordingly (59) approximately becomes

$$\hat{J}_1 \ddot{\varphi} = -c \cdot \varphi - d_\varphi(\mathbf{W}) \cdot \dot{\varphi} \quad \text{if} \quad 0 < \varphi \leq \varphi_l\,, \tag{60}$$

where $c \leq c_\varphi$ is a positive constant (depending on the particular ϑ considered constant during the first phase). We choose

$$d_\varphi(\varphi, \dot{\varphi}, T_\varphi) = \chi^{\varphi_u - \Delta\varphi, \varphi_u}_{\varphi_l, \varphi_l + \Delta\varphi} \left(\varphi, \delta_\varphi, d^*_\varphi(\varphi, \dot{\varphi}, T_\varphi)\right)\,, \tag{61}$$

where δ_φ and $\Delta\varphi < \frac{\varphi_u - \varphi_l}{2}$ are positive constants and the function d^*_φ is discussed further below. It follows from (61) that the damping is rendered constant ($d_\varphi = \delta_\varphi$) for $\varphi \leq \varphi_l$ and for $\varphi \geq \varphi_u$. This has two effects. First, the dynamics (60) are rendered linear, which certainly is a desirable behavior for small alignment errors of the thrust vector. Second, by choosing

$$d_\perp = \delta_\varphi\,, \tag{62}$$

we can ensure that, according to (57), the matrix $\mathbf{D}_{xy}$ becomes constant for small and large values of φ, i.e.

$$\mathbf{D}_{xy} = \delta_\varphi \mathbf{I}_2 > 0 \quad \text{if } \varphi \leq \varphi_l \text{ or } \varphi \geq \varphi_u. \tag{63}$$

This way, difficulties with determining $\mathbf{e}_\varphi$ and $\mathbf{e}_\perp$ near $\varphi = 0$ and $\varphi = \pi$, where $z^2_{dBx} + z^2_{dBy} = 0$, are effectively omitted.

A sophisticated damping strategy d^*_φ is applied in the region $\varphi_l + \Delta\varphi < \varphi < \varphi_u - \Delta\varphi$. There, a strategy similar to the bang-bang solution of a time optimal control is applied. This requires to indicate a switching curve $s_\varphi(\varphi) < 0$, where the transition from acceleration ($\ddot{\varphi} < 0$) to deceleration ($\ddot{\varphi} > 0$) occurs. If $\dot{\varphi} > s(\varphi)$, the damping d^*_φ is chosen to enable maximum acceleration based on (59). In case of $\dot{\varphi} > 0$, this means supporting the torque $-T_\varphi$ by a positive damping

[1] Note that $\varphi = 0$ has to be excluded, since we have defined φ to be positive or equal to zero. Accordingly $\dot{\varphi} \geq 0$ must hold for $\varphi = 0$. The solutions of the given differential equation do not necessarily satisfy this requirement.

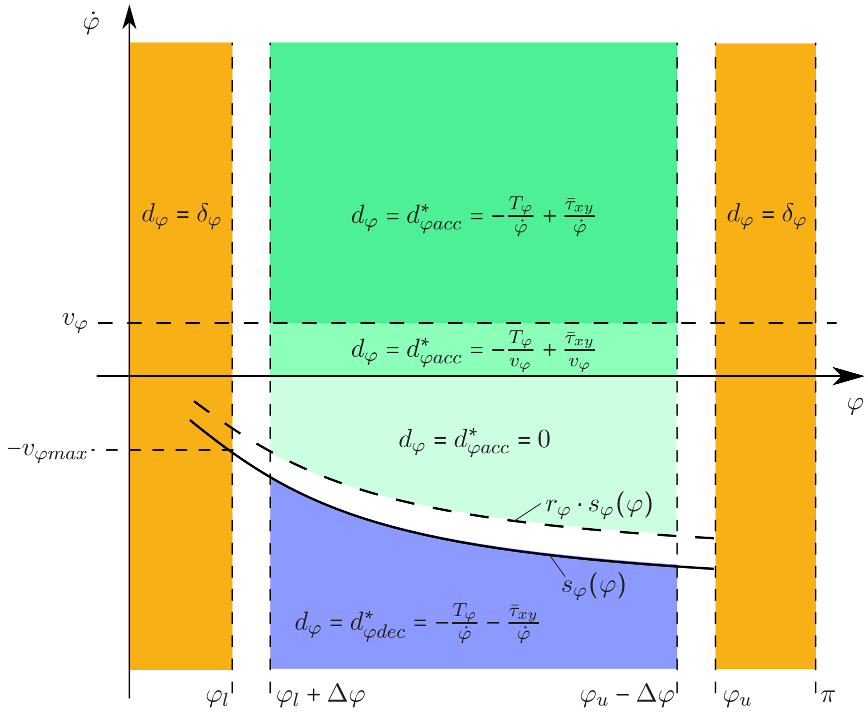

Figure 3: Visualization of the damping $d_\varphi(\varphi, \dot{\varphi}, T_\varphi)$ in the phase plane. Orange areas: Constant damping. Green areas: Acceleration supporting damping. Blue areas: Deceleration supporting damping. White areas indicate regions, where the damping is interpolated.

$d^*_\varphi > 0$, such that the maximum torque $\bar{\tau}_{xy}$ is exploited. In case of $\dot{\varphi} < 0$, the damping is set to zero to avoid counteracting $-T_\varphi$. If $\dot{\varphi} < s(\varphi) < 0$ maximum deceleration is desired, which can be achieved by choosing $d^*_\varphi > 0$ so high that $-T_\varphi$ is overcompensated and $\bar{\tau}_{xy}$ is used to slow down. Summing up, we choose

$$d^*_\varphi(\varphi, \dot{\varphi}, T_\varphi) = \chi^{r_\varphi \cdot s_\varphi(\varphi)}_{s_\varphi(\varphi)}(\dot{\varphi}, d^*_{\varphi dec}(\dot{\varphi}, T_\varphi), d^*_{\varphi acc}(\dot{\varphi}, T_\varphi))\,, \tag{64}$$

where

$$d^*_{\varphi acc}(\dot{\varphi}, T_\varphi) = \begin{cases} -\frac{T_\varphi}{\dot{\varphi}} + \frac{\bar{\tau}_{xy}}{\dot{\varphi}} & \text{if } \dot{\varphi} > v_\varphi\,, \\ -\frac{T_\varphi}{v_\varphi} + \frac{\bar{\tau}_{xy}}{v_\varphi} & \text{if } v_\varphi \geq \dot{\varphi} > 0 \\ 0 & \text{if } 0 \geq \dot{\varphi}\,, \end{cases}, \qquad d^*_{\varphi dec}(\dot{\varphi}, T_\varphi) = -\frac{T_\varphi}{\dot{\varphi}} - \frac{\bar{\tau}_{xy}}{\dot{\varphi}}\,, \tag{65}$$

and r_φ as well as v_φ are positive constants. It is clear from (64) that $0 < r_\varphi < 1$ defines a region of interpolation between $d^*_{\varphi acc}$ and $d^*_{\varphi dec}$ in order to render the resulting torque continuous. An examination of $d^*_{\varphi acc}$ reveals that the small constant $v_\varphi > 0$ prevents the damping from growing unbounded when $\dot{\varphi}$ approaches zero. The switching curve which is used in (64) reads

$$s_\varphi(\varphi) = -\sqrt{v^2_{\varphi max} - 2\hat{J}_1^{-1}\bar{\tau}_{xy}(\varphi_l - \varphi)} < 0\,. \tag{66}$$

This curve is simply the phase-plane trajectory $\dot{\varphi}(\varphi)$ solving the differential equation $\hat{J}_1\ddot{\varphi} = \bar{\tau}_{xy}$ and passing through the point $\dot{\varphi}(\varphi_l) = -v_{\varphi max} < 0$. Figure 3 visualizes the applied damping strategy for d_φ in the phase plane.

The damping d_z is designed analogously to d_φ based on the dynamics

$$\hat{J}_2\ddot{\vartheta} = -|T_z| - d_z(\mathbf{W}) \cdot \dot{\vartheta} \quad \text{if } \vartheta \neq 0\,, \tag{67}$$

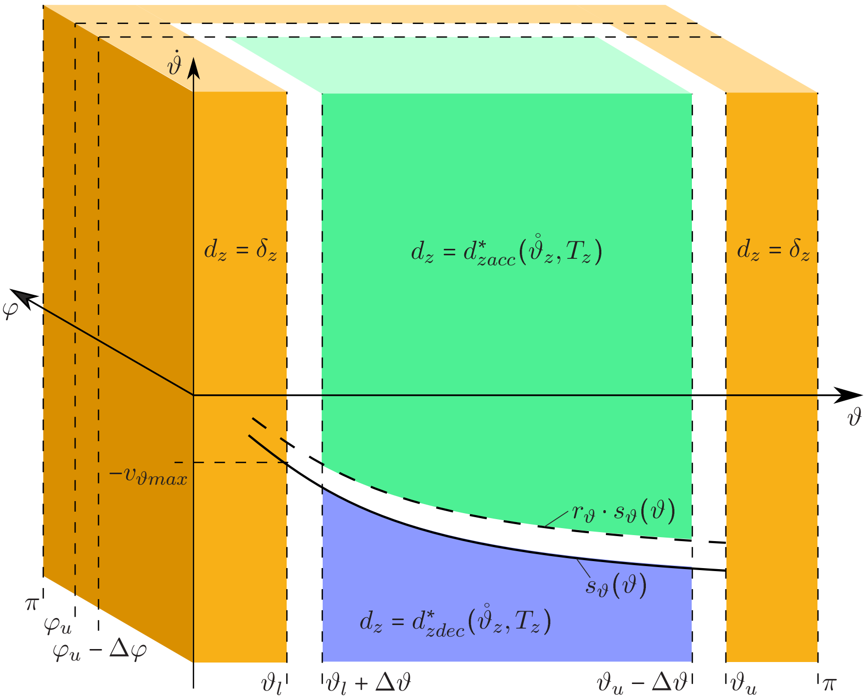

Figure 4: Visualization of the damping $d_z(\varphi, \vartheta, \dot{\vartheta}, \mathring{\vartheta}_z, T_z)$. Orange areas: Constant damping. Green areas: Acceleration supporting damping. Blue areas: Deceleration supporting damping. White areas indicate regions, where the damping is interpolated.

which result from the assumptions that $\kappa_z = 1$ and that the first phase, the alignment of the thrust direction, is completed. Thus $\varphi \equiv 0$ and consequently $\dot{\boldsymbol{\omega}} \parallel \boldsymbol{\omega} \parallel \mathbf{e}_z$ holds. Explicitely, the damping d_z is

$$d_z(\varphi, \vartheta, \dot{\vartheta}, \mathring{\vartheta}_z, T_z) = \chi^{\varphi_u}_{\varphi_u - \Delta\varphi}\left(\varphi, \chi^{\vartheta_u - \Delta\vartheta,\, \vartheta_u}_{\vartheta_l,\, \vartheta_l + \Delta\vartheta}\left(\vartheta, \delta_z, d^*_z(\vartheta, \dot{\vartheta}, \mathring{\vartheta}_z, T_z)\right), \delta_z\right), \tag{68}$$

where $\Delta\vartheta < \frac{\vartheta_u - \vartheta_l}{2}$ and δ_z are positive constants and the quantity $\mathring{\vartheta}_z$ will be introduced later on. Note that the additional outer interpolation function is necessary to account for the non-uniqueness of ϑ if $\varphi = \pi$ and thus serves to satisfy Assumption 1. Figure 4 gives an overview over the damping d_z. The function d^*_z is given by

$$d^*_z(\vartheta, \dot{\vartheta}, \mathring{\vartheta}_z, T_z) = \chi^{r_\vartheta \cdot s_\vartheta(\vartheta)}_{s_\vartheta(\vartheta)}(\dot{\vartheta}, d^*_{zdec}(\mathring{\vartheta}_z, T_z), d^*_{zacc}(\mathring{\vartheta}_z, T_z))\,. \tag{69}$$

The corresponding switching curve is

$$s_\vartheta(\vartheta) = -\sqrt{v^2_{\vartheta max} - 2\hat{J}_2^{-1}\bar{\tau}_z(\vartheta_l - \vartheta)} < 0\,, \tag{70}$$

the damping used for acceleration and deceleration reads

$$d^*_{zacc}(\mathring{\vartheta}_z, T_z) = \begin{cases} -\frac{|T_z|}{\mathring{\vartheta}_z} + \frac{\bar{\tau}_z}{\mathring{\vartheta}_z} & \text{if } \mathring{\vartheta}_z > v_\vartheta\,, \\ -\frac{|T_z|}{v_\vartheta} + \frac{\bar{\tau}_z}{v_\vartheta} & \text{if } v_\vartheta \geq \mathring{\vartheta}_z > 0\,, \\ 0 & \text{if } 0 \geq \mathring{\vartheta}_z\,, \end{cases} \tag{71}$$

$$d^*_{zdec}(\mathring{\vartheta}_z, T_z) = \begin{cases} -\frac{|T_z|}{\mathring{\vartheta}_z} - \frac{\bar{\tau}_z}{\mathring{\vartheta}_z} & \text{if } \mathring{\vartheta}_z < -v_\vartheta\,, \\ -\frac{|T_z|}{-v_\vartheta} - \frac{\bar{\tau}_z}{-v_\vartheta} & \text{if } -v_\vartheta \leq \mathring{\vartheta}_z < 0\,, \\ 0 & \text{if } 0 \leq \mathring{\vartheta}_z\,, \end{cases} \tag{72}$$

and $v_{\vartheta max} > 0$, $v_\vartheta > 0$ and $0 < r_\vartheta < 1$ are constants. Note that we use

$$\mathring{\vartheta}_z = \frac{-x_{dAy}}{\sqrt{1-x_{dAx}^2}}\,\omega_z \tag{73}$$

instead of $\dot{\vartheta}$ to distinguish between the cases in (71) and (72). This is done because d_z is only effective in connection with ω_z and according to (50) the quantity $\mathring{\vartheta}_z$ represents the part of $\dot{\vartheta}$ depending on ω_z. Since $\dot{\vartheta}$ only coincides with $\mathring{\vartheta}_z$ if $\varphi = 0$ or $\omega_\perp = 0$, additional cases have to be distinguished in (71) and (72) compared to (65). This is due to the fact that $\dot{\vartheta}$ and $\mathring{\vartheta}_z$ can have different signs. To clarify this we give one example. Assume that $\dot{\vartheta} < s(\vartheta)$, which means that the error angle is decreasing so fast that maximum deceleration is desired. If $0 \le \mathring{\vartheta}_z$ holds at the same time, the angular rate ω_z already contributes positively to $\dot{\vartheta}$ and accordingly any damping of ω_z would be counterproductive. It follows that $d_z = 0$ is the best choice in that case.

7 Stability Properties

In this section we prove local exponential and almost global asymptotic stability of the desired equilibrium. This is done by showing first that apart from the desired equilibrium further undesired equilibria exist. Local analysis shows that the desired equilibrium is locally exponentially stable and that all undesired equilibria are unstable except for one undesired equilibrium, which can only be shown to be a hyperbolic fixed point. In a second step, using LaSalle's invariance principle we establish instability of the yet unclassified undesired equilibrium and moreover prove that the desired equilibrium exhibits a region of attraction that covers the whole state space except for a manifold of lower dimension than the state space. This type of stability is referred to as almost global asymptotic stability, since according to [12, Appendix B] such a manifold has Lebesgue measure zero. As it is analyzed in [1], almost global asymptotic stability is the best we can achieve with a control law that is continuous over the whole state space.

By inserting the control law (39) derived in the previous section into the open loop dynamics (31), (32) and setting the left hand side to zero, the closed loop equilibrium points can be identified. From (31) one concludes that $\boldsymbol{\omega}_B^{DB} = \mathbf{0}$ must hold and from (32) it is clear that $\tilde{\boldsymbol{\tau}}$ must vanish. Since $\boldsymbol{\omega}_B^{DB} = \mathbf{0}$ the damping plays no role and the equilibrium points are determined by the set, where $\mathbf{T}$ vanishes. With regard to (52) and (41) – (45) two isolated equilibrium points and a connected set of equilibrium points can be established. The two isolated equilibria are

$$\mathbf{W}_d = (\mathbf{I}_3, \mathbf{0})\,, \qquad \mathbf{W}_{u1} = \left(\begin{bmatrix}-\mathbf{e}_x & -\mathbf{e}_y & \mathbf{e}_z\end{bmatrix}, \mathbf{0}\right), \tag{74}$$

where $\mathbf{W}_d$ is the desired equilibrium and $\mathbf{W}_{u1}$ is an undesired equilibrium. The undesired equilibrium $\mathbf{W}_{u1}$ corresponds to the case where the thrust is aligned ($\mathbf{z}_{dB} = \mathbf{e}_z$), whereas the body-fixed x-axis is anti-parallel to its desired orientation ($\mathbf{x}_{dB} = -\mathbf{e}_x$). In terms of $\mathfrak{w}$ these two equilibrium points read

$$\mathfrak{w}_d = \begin{bmatrix}\mathbf{e}_z^T & \begin{bmatrix}1 & 0\end{bmatrix} & \mathbf{0}^T\end{bmatrix}^T, \qquad \mathfrak{w}_{u1} = \begin{bmatrix}\mathbf{e}_z^T & \begin{bmatrix}-1 & 0\end{bmatrix} & \mathbf{0}^T\end{bmatrix}^T \tag{75}$$

and regarding the error angles φ and ϑ it holds that

$$\mathbf{W} = \mathbf{W}_d \implies (\varphi, \vartheta) = (0, 0)\,, \qquad \mathbf{W} = \mathbf{W}_{u1} \implies (\varphi, \vartheta) = (0, \pi)\,. \tag{76}$$

Moreover, every element of the set

$$\mathcal{W}_{u2} = \{\mathbf{W} \in \mathcal{W} : \mathbf{R}_{BD}\mathbf{e}_z = -\mathbf{e}_z, \boldsymbol{\omega}_B^{DB} = \mathbf{0}\} \tag{77}$$

is also an undesired equilibrium point of the closed loop system. It holds that

$$\mathbf{W} \in \mathcal{W}_{u2} \implies \mathbf{z}_{dB} = -\mathbf{e}_z \implies \varphi = \pi\,. \tag{78}$$

Thus, the set $\mathcal{W}_{u2}$ comprises the set of attitudes where the thrust vector is anti-parallel to its desired direction.

7.1 Local Properties

To derive the local properties, the closed loop system is linearized around its equilibrium points. Observe that since $\mathbf{R}_{BD}$ evolves on $SO(3)$ it has only three degrees of freedom. Thus, we can express $\mathbf{R}_{BD}$ locally by three minimal coordinates. In the following we will first express all attitude dependent terms appearing in the closed loop dynamics by a suitable set of local minimal coordinates and then linearize the system in a second step. From Remark 1 we know that $\mathfrak{w}$ is a suitable state representation in a neighborhood of the equilibrium points $\mathbf{W}_d$, $\mathbf{W}_{u1}$ and $\mathfrak{w}_d$, $\mathfrak{w}_{u1}$ respectively. Accordingly, for the linearization around $\mathbf{W}_d$ / $\mathfrak{w}_d$ and $\mathbf{W}_{u1}$ /$\mathfrak{w}_{u1}$ we will use $(\mathbf{z}_{dBxy}, x_{dAy})$ as minimal coordinates representing $(\mathbf{z}_{dB}, \mathbf{x}_{dAxy})$ and thus also $\mathbf{R}_{BD}$.

To deal with the set $\mathcal{W}_{u2}$ we exploit the fact that in a neighborhood of $\mathbf{z}_{dB} = -\mathbf{e}_z \Leftrightarrow \varphi = \pi$ the dynamics of $\mathbf{z}_{dB}$ (which is the last column of $\mathbf{R}_{BD}$) decouple from those of $\mathbf{x}_{dB}$ and $\mathbf{y}_{dB}$ (which are the first two columns of $\mathbf{R}_{BD}$). This can be easily seen by noting that the control law (39) derived in the previous section does depend solely on $\mathbf{z}_{dB}$ and $\boldsymbol{\omega}_B^{DB}$ if $\varphi \geq \varphi_u$. Regarding this decoupled part of the closed loop system given by (33), (35) and (39), the analysis of the set $\mathcal{W}_{u2}$ simplifies to the analysis of the single equilibrium point $(\mathbf{z}_{dB}, \boldsymbol{\omega}_B^{DB})_{u2} = (-\mathbf{e}_z, \mathbf{0})$. Since $\mathbf{z}_{dB} \in \mathcal{S}^2$, it has only two degrees of freedom and we will use $\mathbf{z}_{dBxy}$ as a suitable minimal representation for $\mathbf{z}_{dB}$.

Note that the subsequent linearizations are facilitated by the fact that the damping matrix $\mathbf{D}$ defined in Section 6.2 simplifies to a constant matrix $\mathbf{D} = \mathrm{diag}(\delta_\varphi, \delta_\varphi, \delta_z)$ in a neighborhood of any of the equilibrium points given by (74) and (77).

Local Stability properties of the desired equilibrium $\mathbf{W}_d$ / $\mathfrak{w}_d$

In a neighborhood of $\mathbf{W}_d$ it holds that $\mathbf{z}_{dB} \approx \mathbf{e}_z$ and $\mathbf{x}_{dAxy} \approx \begin{bmatrix} 1 & 0 \end{bmatrix}^T$. Accordingly, $z_{dBz} = \sqrt{1 - (z_{dBx}^2 + z_{dBy}^2)}$ and $x_{dAx} = \sqrt{1 - x_{dAy}^2}$. Inserting this into (33) and (34) yields for the dynamics of $(\mathbf{z}_{dBxy}, x_{dAy})$

$$\begin{bmatrix} \dot{z}_{dBx} \\ \dot{z}_{dBy} \end{bmatrix} = \begin{bmatrix} \omega_{Bz}^{DB} z_{dBy} - \omega_{By}^{DB} \sqrt{1 - (z_{dBx}^2 + z_{dBy}^2)} \\ -\omega_{Bz}^{DB} z_{dBx} + \omega_{Bx}^{DB} \sqrt{1 - (z_{dBx}^2 + z_{dBy}^2)} \end{bmatrix}, \tag{79}$$

$$\dot{x}_{dAy} = -\sqrt{1 - x_{dAy}^2} \left(\frac{z_{dBx} \omega_{Bx}^{DB}}{1 + \sqrt{1 - (z_{dBx}^2 + z_{dBy}^2)}} + \frac{z_{dBy} \omega_{By}^{DB}}{1 + \sqrt{1 - (z_{dBx}^2 + z_{dBy}^2)}} + \omega_{Bz}^{DB} \right). \tag{80}$$

In the dynamics (35) we have to express the attitude dependent terms of $\tilde{\boldsymbol{\tau}}$ by the minimal coordinates. Since in a neighborhood of $\mathbf{W}_d$ a constant damping $\mathbf{D} = \mathrm{diag}(\delta_\varphi, \delta_\varphi, \delta_z)$ is applied only the components of $\mathbf{T}$ given in (52) have to be considered. Recalling that $\varphi \in [0, \pi]$ and hence $\sqrt{z_{dBx}^2 + z_{dBy}^2} = \sin(\varphi)$, the torque $\mathbf{T}_\varphi^\varphi$ can be indicated as

$$\mathbf{T}_\varphi^\varphi = c_\varphi \sin(\varphi) \cdot \mathbf{e}_\varphi = c_\varphi \sin(\varphi) \cdot \frac{1}{\sin(\varphi)} \begin{bmatrix} -z_{dBy} \\ z_{dBx} \\ 0 \end{bmatrix} = c_\varphi \begin{bmatrix} -z_{dBy} \\ z_{dBx} \\ 0 \end{bmatrix}. \tag{81}$$

The torque $\mathbf{T}_\varphi^\vartheta$ can be reformulated using $\sin(\frac{\varphi}{2}) = \sqrt{\frac{1}{2}(1 - \cos(\varphi))}$, $\cos(\frac{\varphi}{2}) = \sqrt{\frac{1}{2}(1 + \cos(\varphi))}$,

$\sin(\varphi) = \sqrt{1-\cos(\varphi)^2} = \sqrt{(1+\cos(\varphi))}\sqrt{(1-\cos(\varphi))}$ and $z_{dBz} = \cos(\varphi)$. One obtains

$$
\begin{aligned}
\mathbf{T}^{\vartheta}_{\varphi} &= c_{\vartheta} \int_0^{\vartheta} \Lambda^{\vartheta_u}_{\vartheta_l}(\zeta)\ d\zeta \cdot \frac{-\left(\sqrt{\frac{1}{2}(1+\cos(\varphi))} - \cos(\frac{\varphi_u}{2})\right)\frac{1}{\sqrt{2}}\sqrt{1-\cos(\varphi)}}{\left(1-\cos(\frac{\varphi_u}{2})\right)^2} \cdot \mathbf{e}_{\varphi} = \\
&= \int_0^{\vartheta} \Lambda^{\vartheta_u}_{\vartheta_l}(\zeta)\ d\zeta \cdot \frac{\frac{-c_{\vartheta}}{\sqrt{2}}\left(\sqrt{\frac{1}{2}(1+\cos(\varphi))} - \cos(\frac{\varphi_u}{2})\right)\sqrt{1-\cos(\varphi)}}{\left(1-\cos(\frac{\varphi_u}{2})\right)^2\sqrt{1+\cos(\varphi)}\sqrt{1-\cos(\varphi)}} \begin{bmatrix} -z_{dBy} \\ z_{dBx} \\ 0 \end{bmatrix} = \\
&= \int_0^{\arccos(x_{dAx})} \Lambda^{\vartheta_u}_{\vartheta_l}(\zeta)\ d\zeta \cdot \frac{\frac{-c_{\vartheta}}{\sqrt{2}}\left(\sqrt{\frac{1}{2}(1+z_{dBz})} - \cos(\frac{\varphi_u}{2})\right)}{\left(1-\cos(\frac{\varphi_u}{2})\right)^2\sqrt{1+z_{dBz}}} \begin{bmatrix} -z_{dBy} \\ z_{dBx} \\ 0 \end{bmatrix} = \\
&= \int_0^{\arccos(\sqrt{1-x^2_{dAy}})} \Lambda^{\vartheta_u}_{\vartheta_l}(\zeta)\ d\zeta \cdot \frac{\frac{-c_{\vartheta}}{\sqrt{2}}\left(\sqrt{\frac{1}{2}\left(1+\sqrt{1-(z^2_{dBx}+z^2_{dBy})}\right)} - \cos(\frac{\varphi_u}{2})\right)}{\left(1-\cos(\frac{\varphi_u}{2})\right)^2\sqrt{1+\sqrt{1-(z^2_{dBx}+z^2_{dBy})}}} \begin{bmatrix} -z_{dBy} \\ z_{dBx} \\ 0 \end{bmatrix}.
\end{aligned}
\tag{82}
$$

Using $\sqrt{1-x^2_{dAx}} = \sin(\vartheta)$ following from $\vartheta \in [0,\pi]$ as well as some properties from above, enables us to write

$$
\begin{aligned}
\mathbf{T}^{\vartheta}_{\perp} &= \frac{\left(\cos(\frac{\varphi}{2}) - \cos(\frac{\varphi_u}{2})\right)^2}{\left(1-\cos(\frac{\varphi_u}{2})\right)^2} \cdot c_{\vartheta}\sin(\vartheta) \cdot \frac{x_{dAy}\sqrt{z^2_{dBx}+z^2_{dBy}}}{\sin(\vartheta)\,(1+z_{dBz})} \cdot \mathbf{e}_{\perp} = \\
&= \frac{c_{\vartheta}\left(\cos(\frac{\varphi}{2}) - \cos(\frac{\varphi_u}{2})\right)^2}{\left(1-\cos(\frac{\varphi_u}{2})\right)^2} \cdot \frac{x_{dAy}\sqrt{z^2_{dBx}+z^2_{dBy}}}{1+z_{dBz}} \cdot \frac{1}{\sqrt{z^2_{dBx}+z^2_{dBy}}} \begin{bmatrix} z_{dBx} \\ z_{dBy} \\ 0 \end{bmatrix} = \\
&= \frac{c_{\vartheta}\left(\sqrt{\frac{1}{2}\left(1+\sqrt{1-(z^2_{dBx}+z^2_{dBy})}\right)} - \cos(\frac{\varphi_u}{2})\right)^2 x_{dAy}}{\left(1-\cos(\frac{\varphi_u}{2})\right)^2\left(1+\sqrt{1-(z^2_{dBx}+z^2_{dBy})}\right)} \begin{bmatrix} z_{dBx} \\ z_{dBy} \\ 0 \end{bmatrix}.
\end{aligned}
\tag{83}
$$

The last component $\mathbf{T}^{\vartheta}_z$ finally reads

$$
\begin{aligned}
\mathbf{T}^{\vartheta}_{z} &= \frac{\left(\cos(\frac{\varphi}{2}) - \cos(\frac{\varphi_u}{2})\right)^2}{\left(1-\cos(\frac{\varphi_u}{2})\right)^2} \cdot c_{\vartheta}\sin(\vartheta) \cdot \frac{x_{dAy}}{\sin(\vartheta)}\ \mathbf{e}_z = \\
&= \frac{c_{\vartheta}\left(\sqrt{\frac{1}{2}\left(1+\sqrt{1-(z^2_{dBx}+z^2_{dBy})}\right)} - \cos(\frac{\varphi_u}{2})\right)^2 x_{dAy}}{\left(1-\cos(\frac{\varphi_u}{2})\right)^2}\ \mathbf{e}_z\ .
\end{aligned}
\tag{84}
$$

For the linearization around $\mathbf{W}_d$ / $\mathfrak{w}_d$, we define the reduced state vector $\mathfrak{w}^d_r = \left[\mathbf{r}^T_d \quad (\boldsymbol{\omega}^{DB}_B)^T\right]^T = \left[z_{dBy} \quad -z_{dBx} \quad -x_{dAy} \quad (\boldsymbol{\omega}^{DB}_B)^T\right]^T$. Note in particular the order and the sign of the first three components. In terms of $\mathfrak{w}^d_r$ the desired equilibrium lies in zero. Linearizing (79) and (80) around $\mathfrak{w}^d_r = \mathbf{0}$ yields

$$
\Delta\dot{\mathbf{r}}_d = \Delta\boldsymbol{\omega}^{DB}_B\ . \tag{85}
$$

The linearization of (35), considering (39), (81), (82), (83), (84) and the constant damping is straight forward but tedious and eventually results in

$$
\Delta\dot{\boldsymbol{\omega}}^{DB}_B = -\mathbf{J}^{-1}\mathbf{C}_d\Delta\mathbf{r}_d - \mathbf{J}^{-1}\mathbf{B}\Delta\boldsymbol{\omega}^{DB}_B\ , \tag{86}
$$

where $\mathbf{C}_d = \mathrm{diag}(c_\varphi, c_\varphi, c_\vartheta) > \mathbf{0}$ and $\mathbf{B} = \mathrm{diag}(\delta_\varphi, \delta_\varphi, \delta_z) > \mathbf{0}$. Combining (85) and (86) yields

$$\Delta\dot{\mathfrak{w}}_r^d = \underbrace{\begin{bmatrix} \mathbf{0} & \mathbf{I}_3 \\ -\mathbf{J}^{-1}\mathbf{C}_d & -\mathbf{J}^{-1}\mathbf{B} \end{bmatrix}}_{\mathbf{A}_d} \Delta\mathfrak{w}_r^d \,. \tag{87}$$

Since $\mathbf{J}^{-1}$ is positive definite, there exists a nonsingular real matrix $\mathbf{M}$, such that $\mathbf{J}^{-1} = \mathbf{M}\mathbf{M}^T$. By defining $\tilde{\mathbf{C}}_d = \mathbf{M}^T\mathbf{C}\mathbf{M} > \mathbf{0}$ and $\tilde{\mathbf{B}} = \mathbf{M}^T\mathbf{B}\mathbf{M} > \mathbf{0}$ one can rewrite $\mathbf{A}_d$ as

$$\mathbf{A}_d = \begin{bmatrix} \mathbf{0} & \mathbf{I}_3 \\ -\mathbf{M}\tilde{\mathbf{C}}_d\mathbf{M}^{-1} & -\mathbf{M}\tilde{\mathbf{B}}\mathbf{M}^{-1} \end{bmatrix} = \begin{bmatrix} \mathbf{M} & \mathbf{0} \\ \mathbf{0} & \mathbf{M} \end{bmatrix} \underbrace{\begin{bmatrix} \mathbf{0} & \mathbf{I}_3 \\ -\tilde{\mathbf{C}}_d & -\tilde{\mathbf{B}} \end{bmatrix}}_{\tilde{\mathbf{A}}_d} \begin{bmatrix} \mathbf{M}^{-1} & \mathbf{0} \\ \mathbf{0} & \mathbf{M}^{-1} \end{bmatrix} . \tag{88}$$

Since the eigenvalues of $\mathbf{A}_d$ and $\tilde{\mathbf{A}}_d$ are the same, we can restrict the analysis to $\tilde{\mathbf{A}}_d$. Let $\mathbf{v} = \begin{bmatrix} \mathbf{v}_1^T & \mathbf{v}_2^T \end{bmatrix}^T$, where $\mathbf{v}_1, \mathbf{v}_2 \in \mathbb{C}^3$, be any eigenvector of $\tilde{\mathbf{A}}_d$ corresponding to the eigenvalue λ. Then, $\tilde{\mathbf{A}}_d\mathbf{v} = \lambda\mathbf{v}$ implies $\mathbf{v}_2 = \lambda\mathbf{v}_1$ and $\tilde{\mathbf{B}}\mathbf{v}_2 + \tilde{\mathbf{C}}_d\mathbf{v}_1 = -\lambda\mathbf{v}_2$. Inserting the first equation into the second yields $\lambda^2\mathbf{v}_1 + \lambda\tilde{\mathbf{B}}\mathbf{v}_1 + \tilde{\mathbf{C}}_d\mathbf{v}_1 = \mathbf{0}$. Multiplying by the complex conjugate $\bar{\mathbf{v}}_1^T$ from the left results in

$$\bar{\mathbf{v}}_1^T\mathbf{v}_1\lambda^2 + \bar{\mathbf{v}}_1^T\tilde{\mathbf{B}}\mathbf{v}_1\lambda + \bar{\mathbf{v}}_1^T\tilde{\mathbf{C}}_d\mathbf{v}_1 = a\lambda^2 + b\lambda + c = 0 \,. \tag{89}$$

From the positive definiteness of $\tilde{\mathbf{C}}_d$ and $\tilde{\mathbf{B}}$ it follows that $a, b, c > 0$ and from the Routh-Hurwitz criterion for polynomials of order two all solutions of (89) lie in the left complex half plane. This proves asymptotic stability of $\mathbf{W}_d$ / $\mathfrak{w}_d$ with local exponential convergence, [11, Theorem 4.15].

Local properties of the undesired equilibrium $\mathbf{W}_{u1}$ / $\mathfrak{w}_{u1}$

In a neighborhood of $\mathbf{W}_{u1}$ it holds that $\mathbf{z}_{dB} \approx \mathbf{e}_z$ and $\mathbf{x}_{dAxy} \approx \begin{bmatrix} -1 & 0 \end{bmatrix}^T$. Accordingly, $z_{dBz} = \sqrt{1 - (z_{dBx}^2 + z_{dBy}^2)}$ still holds and $x_{dAx} = -\sqrt{1 - x_{dAy}^2}$. As a consequence, the dynamics of $\mathbf{z}_{dBxy}$ are still given by (79), whereas the dynamics of x_{dAy} become

$$\dot{x}_{dAy} = \sqrt{1 - x_{dAy}^2}\left(\frac{z_{dBx}\omega_{Bx}^{DB}}{1 + \sqrt{1 - (z_{dBx}^2 + z_{dBy}^2)}} + \frac{z_{dBy}\omega_{By}^{DB}}{1 + \sqrt{1 - (z_{dBx}^2 + z_{dBy}^2)}} + \omega_{Bz}^{DB} \right) . \tag{90}$$

The components of the torque field $\mathbf{T}$ can be computed analogously as before. While $\mathbf{T}_\varphi^\varphi$ is still given by (81), we obtain for the remaining components

$$\mathbf{T}_\varphi^\vartheta = \int\limits_0^{\arccos(-\sqrt{1 - x_{dAy}^2})} \Lambda_{\vartheta_l}^{\vartheta_u}(\zeta)\, d\zeta \cdot \frac{\frac{-c_\vartheta}{\sqrt{2}} \left(\sqrt{\frac{1}{2}\left(1 + \sqrt{1 - (z_{dBx}^2 + z_{dBy}^2)}\right)} - \cos(\frac{\varphi_u}{2}) \right)}{\left(1 - \cos(\frac{\varphi_u}{2})\right)^2 \sqrt{1 + \sqrt{1 - (z_{dBx}^2 + z_{dBy}^2)}}} \begin{bmatrix} -z_{dBy} \\ z_{dBx} \\ 0 \end{bmatrix}, \tag{91}$$

$$\mathbf{T}_\perp^\vartheta = \frac{c_\vartheta \frac{\sin(\vartheta_l)}{\sin(\vartheta_u)} \left(\sqrt{\frac{1}{2}\left(1 + \sqrt{1 - (z_{dBx}^2 + z_{dBy}^2)}\right)} - \cos(\frac{\varphi_u}{2}) \right)^2 x_{dAy}}{\left(1 - \cos(\frac{\varphi_u}{2})\right)^2 \left(1 + \sqrt{1 - (z_{dBx}^2 + z_{dBy}^2)}\right)} \begin{bmatrix} z_{dBx} \\ z_{dBy} \\ 0 \end{bmatrix}, \tag{92}$$

$$\mathbf{T}_z^\vartheta = \frac{c_\vartheta \frac{\sin(\vartheta_l)}{\sin(\vartheta_u)} \left(\sqrt{\frac{1}{2}\left(1 + \sqrt{1 - (z_{dBx}^2 + z_{dBy}^2)}\right)} - \cos(\frac{\varphi_u}{2}) \right)^2 x_{dAy}}{\left(1 - \cos(\frac{\varphi_u}{2})\right)^2} \mathbf{e}_z \,. \tag{93}$$

For the linearization around the undesired equilibrium $\mathbf{W}_{u1}$ / $\mathfrak{w}_{u1}$ another reduced state vector $\mathfrak{w}_r^{u1} = \begin{bmatrix} z_{dBy} & -z_{dBx} & x_{dAy} & (\boldsymbol{\omega}_B^{DB})^T \end{bmatrix}^T$ is defined, where the sign of the third component has been changed. Linearizing around $\mathfrak{w}_r^{u1} = \mathbf{0}$ yields

$$\Delta\dot{\mathfrak{w}}_r^{u1} = \underbrace{\begin{bmatrix} \mathbf{0} & \mathbf{I}_3 \\ -\mathbf{J}^{-1}\mathbf{C}_{u1} & -\mathbf{J}^{-1}\mathbf{B} \end{bmatrix}}_{\mathbf{A}_{u1}} \Delta\mathfrak{w}_r^{u1} \,, \tag{94}$$

where now the equations (80), (90), (81), (91), (92), (93) and the constancy of the damping have been used. Accordingly the stiffness matrix is $\mathbf{C}_{u1} = \mathrm{diag}(c_{u1}, c_{u1}, -c_\vartheta \frac{\sin(\vartheta_l)}{\sin(\vartheta_u)})$, where $c_{u1} = c_\varphi - \frac{c_\vartheta}{2(1-\cos(\frac{\varphi_u}{2}))} \cdot \int_0^\pi \Lambda_{\vartheta_l}^{\vartheta_u}(\xi)d\xi > 0$. As it was shown before, the eigenvalues of $\mathbf{A}_{u1}$ coincide with the eigenvalues of

$$\tilde{\mathbf{A}}_{u1} = \begin{bmatrix} \mathbf{0} & \mathbf{I}_3 \\ -\tilde{\mathbf{C}}_{u1} & -\tilde{\mathbf{B}} \end{bmatrix} , \tag{95}$$

where $\tilde{\mathbf{C}}_{u1} = \mathbf{M}^T\mathbf{C}_{u1}\mathbf{M}$. The eigenvalues of $\tilde{\mathbf{A}}_{u1}$ in turn satisfy

$$\bar{\mathbf{v}}_1^T\mathbf{v}_1\lambda^2 + \bar{\mathbf{v}}_1^T\tilde{\mathbf{B}}\mathbf{v}_1\lambda + \bar{\mathbf{v}}_1^T\tilde{\mathbf{C}}_u\mathbf{v}_1 = a\lambda^2 + b\lambda + c = 0 \,. \tag{96}$$

Note that $\tilde{\mathbf{A}}_{u1}$ obviously has full rank and hence no zero eigenvalues can exist, which implies $c \neq 0$. Moreover, from $\tilde{\mathbf{B}} > 0$ it follows that $b > 0$ and hence no eigenvalues can lie on the imaginary axis. One concludes that $\mathbf{W}_{u1}$ is a hyperbolic fixed point and hence no invariant center manifold $W^c(\mathbf{W}_{u1})$ exists, [12, Appendix B]. It will be proven in the next section that $\mathbf{W}_{u1}$ is unstable and hence an unstable invariant manifold $W^u(\mathbf{W}_{u1})$ of at least dimension one must exist. This in turn limits the stable invariant manifold $W^s(\mathbf{W}_{u1})$ to be of a smaller dimension than the state space.

Local properties of the undesired equilibrium set $\mathcal{W}_{u2}$

As stated before, in a neighborhood of the set $\mathcal{W}_{u2}$, more precisely in the region $\mathcal{U} = \{\mathbf{W} \in \mathcal{W} : \varphi \geq \varphi_u\}$, it suffices to consider the decoupled part of the closed loop dynamics given by (33), (35) and (39). In that region $\mathbf{z}_{dB} \approx -\mathbf{e}_z$ holds and accordingly, using $z_{dBz} = -\sqrt{1-(z_{dBx}^2 + z_{dBy}^2)}$, the dynamics of $\mathbf{z}_{dBxy}$ become

$$\begin{bmatrix} \dot{z}_{dBx} \\ \dot{z}_{dBy} \end{bmatrix} = \begin{bmatrix} \omega_{Bz}^{DB} z_{dBy} + \omega_{By}^{DB}\sqrt{1-(z_{dBx}^2 + z_{dBy}^2)} \\ -\omega_{Bz}^{DB} z_{dBx} - \omega_{Bx}^{DB}\sqrt{1-(z_{dBx}^2 + z_{dBy}^2)} \end{bmatrix} . \tag{97}$$

Since all components of the torque field $\mathbf{T}$ resulting from E_ϑ are zero in that region, i.e. $\mathbf{T}_\varphi^\vartheta = \mathbf{T}_\perp^\vartheta = \mathbf{T}_z^\vartheta = \mathbf{0}$, it remains to consider $\mathbf{T}_\varphi^\varphi$, which is given by

$$\mathbf{T}_\varphi^\varphi = c_\varphi \frac{\sin(\varphi_l)}{\sin(\varphi_u)} \begin{bmatrix} -z_{dBy} \\ z_{dBx} \\ 0 \end{bmatrix} . \tag{98}$$

Defining the reduced state vector $\mathbf{w}_r^{u2} = \begin{bmatrix} -z_{dBy} & z_{dBx} & (\boldsymbol{\omega}_B^{DB})^T \end{bmatrix}^T$ and considering (98) and the constant damping, the linearization of (97) and (35) around $\mathbf{w}_r^{u2} = \mathbf{0}$ yields

$$\Delta\dot{\mathbf{w}}_r^{u2} = \underbrace{\begin{bmatrix} \mathbf{0} & \begin{bmatrix} \mathbf{I}_2 & \mathbf{0} \end{bmatrix} \\ -\mathbf{J}^{-1}\mathbf{C}_{u2} & -\mathbf{J}^{-1}\mathbf{B} \end{bmatrix}}_{\mathbf{A}_{u2}} \Delta\mathbf{w}_r^{u2} \,, \tag{99}$$

where $\mathbf{C}_{u2} = \begin{bmatrix} -c_\varphi \frac{\sin(\varphi_l)}{\sin(\varphi_u)} & 0 \\ 0 & -c_\varphi \frac{\sin(\varphi_l)}{\sin(\varphi_u)} \\ 0 & 0 \end{bmatrix}$. Let $\mathbf{C}_0 = \begin{bmatrix} -c_\varphi \frac{\sin(\varphi_l)}{\sin(\varphi_u)} & 0 & 0 \\ 0 & -c_\varphi \frac{\sin(\varphi_l)}{\sin(\varphi_u)} & 0 \\ 0 & 0 & 0 \end{bmatrix}$ be the matrix which extends $\mathbf{C}_{u2}$ by an additional zero column. By a Laplace expansion along the third column of the matrix $(\lambda \mathbf{I}_6 - \mathbf{A}_0)$, where

$$\mathbf{A}_0 = \begin{bmatrix} \mathbf{0} & \mathbf{I}_3 \\ -\mathbf{J}^{-1}\mathbf{C}_0 & -\mathbf{J}^{-1}\mathbf{B} \end{bmatrix} \tag{100}$$

it can be seen that $\det(\lambda \mathbf{I}_6 - \mathbf{A}_0) = \lambda \det(\lambda \mathbf{I}_5 - \mathbf{A}_{u2})$. Thus, all eigenvalues of $\mathbf{A}_{u2}$ are eigenvalues of $\mathbf{A}_0$, but $\mathbf{A}_0$ has an additional zero eigenvalue. Analogously as before one derives the conditional equation (89), where $\tilde{\mathbf{C}}_d$ is now replaced by the rank two matrix $\tilde{\mathbf{C}}_0 = \mathbf{M}^T \mathbf{C}_0 \mathbf{M} \le \mathbf{0}$. As one can easily verify that $\mathbf{A}_0$ has exactly one zero eigenvalue, the vector $\mathbf{v}_{1,1}$ yielding $c = \bar{\mathbf{v}}_{1,1}^T \tilde{\mathbf{C}}_0 \mathbf{v}_{1,1} = 0$ must be one of the three vectors $\mathbf{v}_{1,i}$, $i \in \{1,2,3\}$, solving $\lambda^2 \mathbf{v}_{1,i} + \lambda \tilde{\mathbf{B}} \mathbf{v}_{1,i} + \tilde{\mathbf{C}}_0 \mathbf{v}_{1,i} = \mathbf{0}$. This can be understood by noting that $c = 0$ in (89) results in $\lambda(\lambda a + b) = 0$, which gives rise to the zero eigenvalue and additionally to a negative eigenvalue $\lambda = -\frac{a}{b}$. Since $\mathbf{A}_0$ has no further zero eigenvalues, $\mathbf{v}_{1,2}$ and $\mathbf{v}_{1,3}$ must be linearly independent of $\mathbf{v}_{1,1}$ and thus yield $c < 0$. It directly follows from $\lambda = \frac{-b \pm \sqrt{b^2 - 4ac}}{2a}$ that $\mathbf{A}_{u2}$ must posses exactly three eigenvalues in the left and two eigenvalues in the right complex half plane. According to [12, Appendix B], in a sufficiently small neighborhood $\mathcal{V} \subset \mathbb{R}^5$ of $\mathbf{w}_r^{u2} = \mathbf{0}$ there exists a local stable invariant manifold $W^s_{\mathbf{w},loc}(\mathbf{0})$ of dimension three and a local unstable invariant manifold $W^u_{\mathbf{w},loc}(\mathbf{0})$ of dimension two. Every point $\mathbf{w}_r^{u2} = \begin{bmatrix} -z_{dBy} & z_{dBx} & (\boldsymbol{\omega}_B^{DB})^T \end{bmatrix}^T \in \mathcal{V}$ corresponds to an one-dimensional compact manifold in the six-dimensional state space $\mathcal{W}$. We denote this manifold by

$$\mathcal{M}(\mathbf{w}_r^{u2}) = \left\{ \mathbf{W} \in \mathcal{W} : \mathbf{W} = (\mathbf{R}_{BD}, \boldsymbol{\omega}_B^{DB}), \mathbf{R}_{BD}\mathbf{e}_z = \begin{bmatrix} z_{dBx} & z_{dBy} & -\sqrt{1 - (z_{dBx}^2 + z_{dBy}^2)} \end{bmatrix}^T \right\}.$$

In particular it holds that $\mathcal{M}(\mathbf{0}) = \mathcal{W}_{u2}$ is the set of the considered undesired equilibrium points. It follows that $W^s_{loc}(\mathcal{W}_{u2}) = \bigcup_{\mathbf{w}_r^{u2} \in W^s_{\mathbf{w},loc}(\mathbf{0})} \mathcal{M}(\mathbf{w}_r^{u2})$ is the four-dimensional local stable invariant manifold of the set $\mathcal{W}_{u2}$. Let $\mathbf{W}(t, \mathbf{W}_0)$ denote the solution of the closed loop system at time t and starting in $\mathbf{W}_0$, i.e. $\mathbf{W}(0, \mathbf{W}_0) = \mathbf{W}_0$. Then the global four-dimensional invariant manifold, which contains all solutions converging to $\mathcal{W}_{u2}$, is $W^s(\mathcal{W}_{u2}) = \bigcup_{t \le 0, \mathbf{W}_0 \in W^s_{loc}(\mathcal{W}_{u2})} \mathbf{W}(t, \mathbf{W}_0)$ [2].

7.2 Global Stability Properties

In this section we prove almost global asymptotic stability of the desired equilibrium following the lines of [8]. Using LaSalle's invariance principle (see e.g. [11, Theorem 4.4]) this is done by showing first that all solutions converge to $\mathbf{W}_d$, $\mathbf{W}_{u1}$ or $\mathcal{W}_{u2}$ and second that the undesired equilibria $\mathbf{W}_{u1}$ and $\mathcal{W}_{u2}$ are only attractive to a set given by an invariant manifold of Lebesgue measure zero.

Recalling that all level sets of V are positively invariant and compact, we apply LaSalle's invariance principle by showing that the set $\mathcal{E} := \{\mathbf{W} \in \mathcal{W} : \dot{V}(\mathbf{W}) = 0\}$ contains no invariant sets apart from the set of equilibrium points $\{\mathbf{W}_d, \mathbf{W}_{u1}, \mathcal{W}_{u2}\}$. Inserting (56) in (40) and using (55) yields

[2] While the vector field of the closed loop system is forward complete, the existence of the solutions for all $t \in \mathbb{R}_-$ is not guaranteed. Although the somewhat sloppy expression $t \le 0$ is intuitive, one should more precisely add $t \in \mathcal{I}(\mathbf{W}_0)$, where $\mathcal{I}(\mathbf{W}_0)$ is the maximal interval of existence for the solution starting in $\mathbf{W}_0$. Compare also [12, Appendix B]

$$\dot{V}(\mathbf{W}) = -\kappa_{xy}(\mathbf{W})\left(d_\varphi(\mathbf{W})\omega_\varphi^2 + d_\perp\omega_\perp^2\right) - \kappa_z(\mathbf{W})d_z(\mathbf{W})\omega_z^2 \,. \tag{101}$$

Taking into account that $\kappa_{xy}, \kappa_z > 0$ the derivative $\dot{V}$ only vanishes if $d_\varphi(\mathbf{W})\omega_\varphi^2 = d_\perp\omega_\perp^2 = d_z(\mathbf{W})\omega_z^2 = 0$ holds. Outside the equilibrium points, in the set $\tilde{\mathcal{W}} = \mathcal{W}\backslash\{\mathbf{W}_d, \mathbf{W}_{u1}, \mathcal{W}_{u2}\}$, this condition is only fulfilled in the subset $\mathcal{E}_1$, which is the set of all states with zero angular velocity, and in the sets $\mathcal{E}_2$, $\mathcal{E}_3$, $\mathcal{E}_4$, in which $\boldsymbol{\omega}_B^{DB} \neq \mathbf{0}$ while $\omega_\perp = d_\varphi(\mathbf{W})\omega_\varphi^2 = d_z(\mathbf{W})\omega_z^2 = 0$. Thus, the sets $\mathcal{E}_2$, $\mathcal{E}_3$, $\mathcal{E}_4$ are subsets of the state space regions where $d_\varphi(\mathbf{W}) = 0$ or $d_z(\mathbf{W}) = 0$ holds. In view of (61) and (68) a necessary condition for this to happen is $\varphi \in \Phi = \{\varphi : \varphi_l + \Delta\varphi \le \varphi \le \varphi_u - \Delta\varphi\}$ or $\vartheta \in \Theta = \{\vartheta : \vartheta_l + \Delta\vartheta \le \vartheta \le \vartheta_u - \Delta\vartheta\}$. Explicitly stated, the sets $\mathcal{E}_1$, $\mathcal{E}_2$, $\mathcal{E}_3$, $\mathcal{E}_4$ are

$$\mathcal{E}_1 = \left\{\mathbf{W} \in \tilde{\mathcal{W}} : \boldsymbol{\omega}_B^{DB} = \mathbf{0}\right\}, \tag{102}$$

$$\mathcal{E}_2 = \left\{\mathbf{W} \in \tilde{\mathcal{W}} : \varphi \in \Phi,\ \vartheta \in \Theta,\ r_\varphi s_\varphi(\varphi) \le \dot{\varphi} \le 0,\ r_\vartheta s_\vartheta(\vartheta) \le \mathring{\vartheta}_z \le 0,\ \dot{\varphi} + \mathring{\vartheta}_z \neq 0,\ \omega_\perp = 0\right\}, \tag{103}$$

$$\mathcal{E}_3 = \left\{\mathbf{W} \in \tilde{\mathcal{W}} : \varphi \in \Phi,\ \vartheta \notin \Theta,\ r_\varphi s_\varphi(\varphi) \le \dot{\varphi} < 0,\ \omega_\perp = 0,\ \omega_z = 0\right\}, \tag{104}$$

$$\mathcal{E}_4 = \left\{\mathbf{W} \in \tilde{\mathcal{W}} : \varphi < \varphi_l + \Delta\varphi,\ \vartheta \in \Theta,\ r_\vartheta s_\vartheta(\vartheta) \le \mathring{\vartheta}_z < 0,\ \omega_\perp = 0,\ \omega_\varphi = 0\right\}. \tag{105}$$

Note that $\omega_\varphi = -\dot{\varphi}$ as well as $\omega_z = -\frac{\sqrt{1-x_{dAx}^2}}{x_{dAy}}\mathring{\vartheta}_z$ holds and consequently $\boldsymbol{\omega}_B^{DB} \neq \mathbf{0}$ in $\mathcal{E}_2 \cup \mathcal{E}_3 \cup \mathcal{E}_4$. Moreover, since $\omega_\perp = 0$ it follows from (73) and (50) that $\mathring{\vartheta}_z = \dot{\vartheta}$ and accordingly $\omega_z = -\frac{\sqrt{1-x_{dAx}^2}}{x_{dAy}}\dot{\vartheta}$.

Next, we show that $\{\mathbf{W}_d, \mathbf{W}_{u1}, \mathcal{W}_{u2}\}$ is the largest invariant set contained in $\mathcal{E} = \mathcal{E}_1 \cup \mathcal{E}_2 \cup \mathcal{E}_3 \cup \mathcal{E}_4 \cup \{\mathbf{W}_d, \mathbf{W}_{u1}, \mathcal{W}_{u2}\}$.

Imagine that $\mathbf{W} \in \mathcal{E}_1$, then $\tilde{\boldsymbol{\tau}} \neq \mathbf{0}$ and since $\boldsymbol{\omega}_B^{DB} = \mathbf{0}$, we have $\dot{\boldsymbol{\omega}}_B^{DB} \neq \mathbf{0}$ from (32). Thus, the state will exit the subset $\mathcal{E}_1$ instantaneously, which shows that no invariant sets are contained in $\mathcal{E}_1$.

We proceed by showing that no invariant sets are contained in $\mathcal{E}_2$. As long as the state of the closed loop system is inside the subset $\mathcal{E}_2$, it follows from (55) that

$$\boldsymbol{\omega}_B^{DB} = -\dot{\varphi}\,\mathbf{e}_\varphi - \frac{\sqrt{1 - x_{dAx}^2}}{x_{dAy}}\dot{\vartheta}\,\mathbf{e}_z \neq \mathbf{0} \,. \tag{106}$$

A lower bound $\underline{\omega}$ for the angular velocity can be derived solving

$$E_{rot0} = \frac{1}{2}(\boldsymbol{\omega}_{B0}^{DB})^T\mathbf{J}\boldsymbol{\omega}_{B0}^{DB} = \frac{1}{2}\bar{\lambda}(\mathbf{J})\underline{\omega}^2 > 0 \,, \tag{107}$$

where $\bar{\lambda}(\mathbf{J})$ denotes the largest eigenvalue of $\mathbf{J}$, E_{rot0} is the rotational energy and $\boldsymbol{\omega}_{B0}^{DB}$ the angular velocity at the time $t = 0$. Since in the set $\mathcal{E}_2$ no damping occurs, using (52) the torque can be identified as $\tilde{\boldsymbol{\tau}} = \mathbf{T} = \mathbf{T}_\varphi^\varphi + \mathbf{T}_\varphi^\vartheta + \mathbf{T}_\perp^\vartheta + \mathbf{T}_z^\vartheta = k_\varphi \cdot \mathbf{e}_\varphi + k_\perp \cdot \mathbf{e}_\perp + \frac{x_{dAy}}{\sqrt{1-x_{dAx}^2}}k_z \cdot \mathbf{e}_z$ with $k_\varphi > 0$ and $k_z > 0$. Now as long as $\mathbf{W} \in \mathcal{E}_2$, it holds that $\dot{E}_{rot} = (\boldsymbol{\omega}_B^{DB})^T\tilde{\boldsymbol{\tau}} = -\dot{\varphi}k_\varphi - \dot{\vartheta}k_z > 0$ and consequently

$$\underline{\omega}^2 \le (\boldsymbol{\omega}_B^{DB})^T\boldsymbol{\omega}_B^{DB} = \dot{\varphi}^2 + \dot{\vartheta}^2 \,. \tag{108}$$

Based on (66) and (70), a lower bound for $\dot{\varphi}$ and $\dot{\vartheta}$ is given by

$$-L = \min(s_\varphi(\pi), s_\vartheta(\pi)) < \min(\dot{\varphi}, \dot{\vartheta}) < 0. \tag{109}$$

Making use of (109), we can hence extend (108) to obtain

$$\underline{\omega}^2 \le \dot{\varphi}^2 + \dot{\vartheta}^2 < -L(\dot{\varphi} + \dot{\vartheta}). \tag{110}$$

Now, let $\varphi_0 \in \Phi$ and $\vartheta_0 \in \Theta$ be the error angles at $t = 0$. The time $\tilde{t}$ solving the equation

$$(\varphi_l + \Delta\varphi) + (\vartheta_l + \Delta\vartheta) = (\varphi_0 + \vartheta_0) + \int_0^{\tilde{t}} (\dot{\varphi} + \dot{\vartheta}) dt \tag{111}$$

certainly is an upper bound of the time at which the state must leave $\mathcal{E}_2$ at the latest. By inserting (110) in (111) and evaluating the integral, we obtain the inequality

$$(\varphi_l + \Delta\varphi) + (\vartheta_l + \Delta\vartheta) \le (\varphi_0 + \vartheta_0) - \frac{\underline{\omega}^2}{L}\tilde{t}, \tag{112}$$

which reveals that $\tilde{t}$ itself is upper bounded by

$$\tilde{t} \le L \frac{(\varphi_0 - (\varphi_l + \Delta\varphi)) + (\vartheta_0 - (\vartheta_l + \Delta\vartheta))}{\underline{\omega}^2}. \tag{113}$$

Accordingly, $\mathcal{E}_2$ is left in any case and cannot contain any invariant sets. The same holds true for $\mathcal{E}_3$ and $\mathcal{E}_4$. This can be shown by proceeding completely analogously as before and is therefore omitted here. Moreover, also the union of $\mathcal{E}_1$, $\mathcal{E}_2$, $\mathcal{E}_3$ and $\mathcal{E}_4$ cannot contain any invariant sets. Indeed, the state may cross over from $\mathcal{E}_1$ into each of the other sets and also from $\mathcal{E}_2$ to $\mathcal{E}_3$ or $\mathcal{E}_4$ but no other transitions are possible. Hence, the union of the sets of equilibrium points $\{\mathbf{W}_d, \mathbf{W}_{u1}, \mathcal{W}_{u2}\}$ is the largest invariant set contained in $\mathcal{E}$ and according to LaSalle's invariance principle every trajectory converges to $\mathbf{W}_d$, $\mathbf{W}_{u1}$ or $\mathcal{W}_{u2}$.

In order to prove almost global asymptotic stability of $\mathbf{W}_d$ we first notice that $V(\mathbf{W}_d) = 0$, $V(\mathbf{W}_{u1}) = E_\vartheta(0,\pi) > 0$ and $V(\mathbf{W}) = E_\varphi(\pi) > 0$, $\forall \mathbf{W} \in \mathcal{W}_{u2}$. It follows from (41) and (43) that $E_\varphi(\pi) = \max(E_{pot}(\varphi,\vartheta))$ and consequently $E_\vartheta(0,\pi) < E_\varphi(\pi)$. If we choose any initial state $\mathbf{W}_0$, such that $V(\mathbf{W}_0) < E_\vartheta(0,\pi)$, we exclude $\mathbf{W}_{u1}$ and $\mathcal{W}_{u2}$ from the initial sublevel set of V and the solution can only approach $\mathbf{W}_d$. Hence, $\mathbf{W}_d$ is an asymptotically stable equilibrium point. Since the set $\{\mathbf{W} \in \mathcal{W} : V(\mathbf{W}) < E_\vartheta(0,\pi)\}$ is adjacent to $\mathbf{W}_{u1}$, the preceding argumentation also proves that $\mathbf{W}_{u1}$ is an unstable equilibrium and according to the analysis in Section 7.1 its stable invariant manifold $W^s(\mathbf{W}_{u1})$ must be of smaller dimension than the state space, i.e. $\dim(W^s(\mathbf{W}_{u1})) < 6$. From the analysis of $\mathcal{W}_{u2}$ in Section 7.1 we moreover know that all solutions converging to $\mathcal{W}_{u2}$ are contained in the stable invariant manifold $W^s(\mathcal{W}_{u2})$, which is of dimension four. Accordingly, the set of undesired equilibria $\{\mathbf{W}_{u1}, \mathcal{W}_{u2}\}$ only attracts solutions along the invariant manifold $W^s(\mathbf{W}_{u1}) \cup W^s(\mathcal{W}_{u2})$, which is of smaller dimension than the state space. It is known that an m-dimensional invariant manifold of an n-dimensional system has Lebesgue measure zero if $m < n$, see e.g. [12, Appendix B]. This proves almost global asymptotic stability of $\mathbf{W}_d$.

8 Conclusion

In this paper we have presented an energy based attitude tracking controller for a quadrotor helicopter. The proposed controller prioritizes the alignment of the thrust axis compared to the heading and thus considers the significance of the thrust axis for the translational motion of a quadrotor helicopter. On the one hand the nonlinear controller is a direct extension of the reduced attitude tracking controller presented in [7]. On the other hand it can also be perceived as an extension of the attitude setpoint controller presented in [8] that involves the addition of feedforward terms to the control law as well as some modifications of the potential energy. Since the closed loop error dynamics of the tracking control problem and the setpoint control problem are very similar, we refer the interested reader to [8] for a performance analysis based on simulation results. Compared to [8] the control problem has been additionally reformulated using the rotation matrix as the attitude representation of choice. Hereby, the ambiguity of the quaternion representation is omitted. It has been proven that the equilibrium of the closed loop dynamics, indicating a zero tracking error, is locally exponentially and almost globally asymptotically stable.

References

[1] S. P. Bhat and D. S. Bernstein. A topological obstruction to continuous global stabilization of rotational motion and the unwinding phenomenon. *Systems & Control Letters*, 39(1):63–70, January 2000.

[2] F. Bullo, R. M. Murray, and A. Sarti. Control on the sphere and reduced attitude stabilization. Technical report, California Institute of Technology, 1995.

[3] P. Castillo, P. Albertos, P. Garcia, and R. Lozano. Simple real-time attitude stabilization of a quad-rotor aircraft with bounded signals. In *Proc. Conference on Decision and Control*, pages 1533 –1538, 2006.

[4] N. A. Chaturvedi, N. H. McClamroch, and D. S. Bernstein. Asymptotic smooth stabilization of the inverted 3d pendulum. *IEEE Trans. Automat. Contr.*, 54:1204 – 1215, June 2009.

[5] N. A. Chaturvedi, A. K. Sanyal, and N. H. McClamroch. Rigid body attitude control. *IEEE Control Syst. Mag.*, 31:30 – 51, June 2011.

[6] L. Derafa, A. Benallegue, and L. Fridman. Super twisting control algorithm for the attitude tracking of a four rotors uav. *Journal of the Franklin Institute*, October 2011.

[7] O. Fritsch. *Methoden und Anwendungen der Regelungstechnik, Erlangen-Münchener Workshops 2011 und 2012*, chapter Fast Tracking Control for the Thrust Direction of a Quadrotor Helicopter. Shaker, Aachen, 2013.

[8] O. Fritsch, B. Henze, and B. Lohmann. Fast and saturating attitude control for a quadrotor helicopter. In *Proc. European Control Conference*, 2013.

[9] Oliver Fritsch, Bernd Henze, and Boris Lohmann. Fast and saturating thrust direction control for a quadrotor helicopter. *at - Automatisierungstechnik*, 61(3):172–182, March 2013.

[10] M.-D. Hua, T. Hamel, P. Morin, and C. Samson. A control approach for thrust-propelled underactuated vehicles and its application to VTOL drones. *IEEE Trans. Automat. Contr.*, 54(8):1837–1853, Aug. 2009.

[11] H.K. Khalil. *Nonlinear systems*. Prentice Hall, Upper Saddle River, NJ, 3-rd edition, 2002.

[12] M. Krstic, J. W. Modestino, and H. Deng. *Stabilization of Nonlinear Uncertain Systems*. Springer, New York, 1998.

[13] T. Lee. Geometric tracking control of the attitude dynamics of a rigid body on so(3). In *Proc. American Control Conference*, pages 1200–1205, 2011.

[14] R. Ortega, A.J. Van Der Schaft, I. Mareels, and B. Maschke. Putting energy back in control. *IEEE Control Syst. Mag.*, 21(2):18–33, 2001.

[15] M. Shuster. A survey of attitude representations. *The Journal of the Astronautical Sciences*, 41(4):439–517, 1993.

[16] A. Tayebi and S. McGilvray. Attitude stabilization of a vtol quadrotor aircraft. *IEEE Trans. Contr. Syst. Technol.*, 14(3):562–571, May 2006.

[17] P. Tsiotras and J. M. Longuski. Spin-axis stabilization of symmetric spacecraft with two control torques. *Systems & Control Letters*, 23:395 – 404, 1994.